NASA TM-88195

NASA Technical Memorandum 88195

NASA-TM-88195 19860018587

Experimental Study of Flow Deflectors Designed to Alleviate Ground Winds Induced by Exhaust of 80-by 120-Foot Wind Tunnel

Vernon J. Rossow, Gene I. Schmidt, Michael S. Reinath, Johannes M. Van Aken, Cynthia L. Parrish and Raymond F. Schuler

January 1986

NF01658

NASA

National Aeronautics and
Space Administration

NASA Technical Memorandum 88195

Experimental Study of Flow Deflectors Designed to Alleviate Ground Winds Induced by Exhaust of 80-by 120-Foot Wind Tunnel

Vernon J Rossow,
Gene I. Schmidt,
Michael S Reinath, Ames Research Center, Moffett Field, California
Johannes M. Van Aken, University of Kansas, Lawrence, Kansas
Cynthia L. Parrish,
Raymond F. Schuler, Ames Research Center, Moffett Field, California

January 1986

NASA

National Aeronautics and
Space Administration

Ames Research Center
Moffett Field, California 94035

EXPERIMENTAL STUDY OF FLOW DEFLECTORS DESIGNED TO ALLEVIATE GROUND WINDS INDUCED BY EXHAUST OF 80- BY 120-FOOT WIND TUNNEL

Vernon J. Rossow, Gene I. Schmidt, Michael S. Reinath, Johannes M. Van Aken*,
Cynthia L. Parrish, and Raymond F. Schuler

Ames Research Center

SUMMARY

A description is presented of an experimental study directed at finding a deflector ramp that will reduce to an acceptable level the ground winds under the exhaust jet of the 80- by 120-Foot Wind Tunnel at NASA Ames Research Center. A one-fiftieth-scale model of the full-scale facility was used to investigate how the jet flow field was modified by the various design parameters of the ramp. It was concluded that the ground winds were alleviated sufficiently by a ramp with end plates located next to the wind tunnel building along the ground edge of the exhaust opening. At full scale, the ramp should have a slant length of 7.62 m (25 ft) or more, and would be elevated at about 45° to the ground plane. The material should have holes less than 15.2 cm (6 in.) in diameter distributed uniformly over its surface to produce a porosity of about 30%.

INTRODUCTION

The National Full-Scale Aerodynamics Complex (NFAC) at NASA Ames Research Center consists of a 40- by 80-Foot Wind Tunnel and an 80- by 120-Foot Wind Tunnel, both of which share a portion of their circuits so they can use the same drive system (figs. 1 and 2). Background studies (refs. 1-6), carried out prior to the design and construction of NFAC, considered a variety of configurations that pointed to the need for certain desirable characteristics in the facilities. When tests were begun in 1982 that would lead to implementation of the wind tunnels, various features or parts of the facility were identified as in need of modification or additional structure. An overview of these redesign and modification efforts is presented in reference 7. The portion of NFAC which is being considered in this paper, and which is in need of additional structure, is the region where the 80 by 120 airstream exhausts into the atmosphere (figs. 1 and 2). In particular, the problem to be treated is the reduction of the high winds near the ground in and around the exhaust jet at the south end of the facility. The investigation to be reported here was directed at finding changes in or additions to the structure which would reduce the magnitude of the induced ground winds to a level which does not interfere with the usual activities in the area.

---

*University of Kansas, Lawrence, KS 66044

DESCRIPTION OF PROBLEM

The operation of a wind tunnel of the flow-through type requires that air be drawn from the atmosphere into the circuit through a specially tailored entry region which adapts the airstream to the flow quality desired for the test section (refs. 1-8). After the air passes through the test section and drive fans, it is exhausted back into the atmosphere through openings at the end of the facility. Insufficiencies in the design of either end of the circuit can have a significant adverse effect on the utility of the facility. The disadvantages over a facility of the closed-circuit type are offset by, for example, the ability to run continuously with highly powered models in a larger test section with less drive-fan power. It is necessary then to achieve an acceptable design at both the inlet and the exhaust ends of flow-through wind tunnels.

As mentioned in the Introduction, tests that were carried out in 1982 to implement the NFAC indicated that unacceptably high winds were present near the exhaust of the 80 by 120. Measurements taken on the ground under the exhaust jet with a hand-held wind anemometer (fig. 3) showed that the region was unsteady, with wind gusts in excess of the velocity of the jet. The high wind velocities and turbulence near the ground and around nearby buildings were believed to be caused by the winds induced at the edges of the jet.

Before consideration is given to modifying the exhaust region to alleviate the winds around the jet, the nature of the exhaust opening and nearby surfaces are described as is the role they might have in the structure of the jet as it leaves the building. As shown in figure 2(b), the eastern half of the south wall of the 40- by 80-Foot Wind Tunnel building is permanently closed. The western half of the south wall is composed of door panels arranged in 12 rows and 9 columns, and is referred to as vane set #7. It is to be noted in figure 2(b) that three doors were left off in the westernmost column during the 1982 tests. These permanent openings provide exhaust ports for the air-exchange system used to cool the 40 by 80 during the 1982 tests. The rest of the door panels are closed for the operation of the 40 by 80 and are opened for the operation of the 80 by 120. When vane set #7 is open, the panels swing inward to avoid the superstructure and a bird/debris screen which is attached to the outside of the building (figs. 2(b) and 4). Each row of panels is set to swing inward at varying degrees so that the doors deflect the exhaust airstream upward at different angles as illustrated in figure 4. The intent of the splay was to accelerate the disperson of the jet after it leaves the building. The original designs of NFAC called for a ramp or ground-based structure to be added outside the building to help deflect the bottom of the jet off the ground, but such a unit was not built because of a shortage of funds. Whether such a ramp is necessary or whether another set of deflectors added to vane set #7 would effectively deflect the air is uncertain. The presence of the screen and superstructure at the trailing edges of the door panels suggests, however, that their lifting effectiveness is reduced and an external ramp or deflector is required.

Internal structures which probably cause some nonuniformities and small-scale turbulence in the jet are vane set #6, with four vanes nearest the corner offset to accommodate vane set #7 as it swings inward; a 4-ft step from the floor of the tunnel up to ground level outside the tunnel; and the walls of the west leg of the tunnel which confine the flow between the six drive fans and vane set #6 (figs. 1 and 5). Substantial changes in any or all of these items would not only be difficult to implement, but any new arrangement would probably not cause a significant change in the jet structure or in the ground winds induced by the jet. The only item studied in the investigation was the 4-ft step from the inside floor leading up to the outside ground level (fig. 4). A fairing on the inside of the tunnel did not measurably alter the induced ground winds, nor did such a step alter the effectiveness of the ramp deflector recommended in the next section as a solution to the ground wind problem.

It was therefore concluded that the present investigation should be directed at a determination of the best size, shape, and location for a deflector ramp at or near the ground just outside the exhaust opening. The use of a ground-mounted (rather than a side- or roof-mounted) ramp similar to those indicated in references 1-6 is the most effective location because it is nearest to the problem area. It was also reasoned that the ramp material should be porous rather than solid to allow a small amount of the exhaust air to pass on through while most is deflected upward. If the ramp is solid or nonporous, all of the jet is deflected upward so that a flow is induced toward the building as shown in figure 6(b); but if the porosity of the ramp is too large, air passes readily through the ramp to produce winds away from the building as shown in figure 6(a). When the porosity is somewhere between these two situations, a balance is reached in which the oppositely directed winds cancel each other as shown in figure 6(c). These two-dimensional considerations do not treat problems which may occur at the sides of the jet. It remains then to experimentally determine the proper porosity, size, shape, and configuration, and location of the deflector ramp which provides the greatest alleviation of the winds below the jet.

OVERVIEW OF EXPERIMENTAL PROGRAM

As stated in the previous section, the objective of the experimental program is to define a range of design parameters for a deflector ramp that will reduce the velocity of the ground winds to an acceptable level. An acceptable level is defined here as a level in which the induced velocities are 10% or less of the jet center-line velocity (which is slightly less than half of the test section velocity). The parameters which are used to describe the deflector and which will be varied in the experiments are

1. Length

2. Shape (curved or flat)

3. Angle of inclination relative to the ground plane

4. Porosity (also, distribution of porosity; e.g., uniform or nonuniform)

5. Location relative to exhaust opening

6. End configuration

This list assumes that the ramp will essentially be constant in shape across the opening (i.e., two-dimensional), with perhaps some sort of cap or plate at the two ends. A list of the ramp designs tested is presented in table 1.

The device to be used to evaluate the various deflector ramps is the one-fiftieth-scale model (fig. 7) of the NFAC facility (Smith, Schmidt, Van Aken, and Parish; NASA TM in preparation). The model replicates most of the features of the full-scale facility. Those characteristics (such as corrugated wall cladding) which become impractically small when reduced in size by a factor of 50 were not incorporated into the model. Some structural components were simulated in an approximate fashion with screens or roughness. For example, the structural beams and the bird/debris screen has a mesh spacing of 1.9 cm by 1.9 cm with 0.27-cm-diam wire (a 0.75-by 0.75-in. mesh with 0.105-in.-diam wire) were constructed to yield a porosity of 73.9% and an estimated loss coefficient of 0.432. The screen is attached to the outside of the south wall (figs. 2 and 4) was simulated on the model tunnel with a brass screen (14×16 mesh with 0.264-mm-diam (0.0104-in.) wire, porosity = 71%) estimated to have a pressure drop across it approximately the same as the two items together. The size and deflection of the doors of vane set #7 in the open position were replicated (fig. 4), but the corrugations on one side and the interference of the edges of the beams were not.

Since the Reynolds number of the model components is over 50 times smaller than full scale, questions arise as to how well the aerodynamics of the model matches the full-scale result. Cases in which a direct comparison could be made between the two facilities produced quite good agreement (ref. 7). As expected, small differences occurred in the losses across the vane sets and in other places where the spread in Reynolds number could cause significant differences in the flow.

Of interest here is the quality of the representation of the exhaust-jet flow field outside the building. An attempt was first made to measure the velocity magnitudes and directions under the exhaust of the model on a ground plane to compare with the full-scale results presented in figure 3. Confirmation was achieved at a few locations near the edges of the jet, but the flow was so unsteady and the space was so limited between the jet and the ground plane that other reliable measurements could not be made. These results were then supplemented with an oil-smear run to obtain an estimate of the streamline pattern on the ground plane. The resulting pattern, presented in figure 8, is quite similar to the velocity-vector pattern presented in figure 3 for the full-scale facility. The general pattern and the small reversed-flow region next to the building and under the center of the jet are noted to be alike in both figures. Both are averaged steady-state results right on the ground plane. The data taken with the hand-held anemometer were averaged over part of a minute and the oil-streak pattern was obtained by running the tunnel for about 0.5 hr after a thin layer of oil had been brushed onto the ground plane.

This comparison and the other satisfactory comparisons between model and full-scale led to the conclusion that the model was acceptable as a screening device for the study of deflector-ramp designs.

Even though the foregoing results with the hand-held anemometer, pitot tubes, and oil smears were qualitatively correct, other more accurate and rapid means had to be used to determine whether a particular ramp design was satisfactory. For this reason, an extensive array of yarn tufts was attached to the ground plane and to the roof of a representation of a nearby building under and around the exhaust jet. A hand-held tuft wand and a smoke wand (using a mixture of SO_2 and NH_3) were used to visualize the flow patterns that were generated. Although these two methods gave a quick, accurate evaluation of ramp configurations, the most satisfactory and quantitative measurement technique was obtained with a Laser Velocimeter (LV) unit (refs. 9 and 10). The instrument measures two components of the velocity at points anywhere between 2.3 m (7.5 ft) and 10 m (33 ft) from the output lens. Since the cross-stream velocity component was small and had a secondary effect on the flow at the ground plane, this component was not measured. The LV instrument was therefore located to the side of the jet (fig. 11 of ref. 10) so that the two measured components consisted of the vertical and the horizontal component in the direction perpendicular to exhaust opening (i.e., the south wall of the building). As a consequence, the flow field of the exhaust jet and the surrounding air motions could be defined quite accurately. The LV is ideally suited to this problem because it makes a remote, nonintrusive measurement which is accurate on both large and small velocities.

The velocity distribution was measured with the LV on a point-by-point basis at a given station along a vertical or horizontal survey line. Once the flow in the model tunnel was established and brought to steady state (dynamic pressure in test section = $q_{ts} \approx 479$ N/m^2 (10 lb/ft^2), $V_{ts} \approx 28$ m/sec (92 ft/sec)), data were taken at a desired point in the flow field. The flow was seeded upstream of the measuring point with an aerosol oil mist to enhance the data-taking rate of the LV. The velocity components of the oil mist droplets passing through the focal volume were accumulated to form a velocity histogram of 100 data points. An average (or mean) and σ (the estimator of standard deviation) were then calculated. On the basis of those values, any data samples that deviated by more than 3σ from the mean were discarded. New values for the mean and for σ were then recomputed and used to calculate the parameter

$$\Delta V = \pm \sigma z_c / \sqrt{N} \qquad (1)$$

where ΔV is the uncertainty interval about the mean velocity corresponding to a 95% confidence level, σ is the estimator of standard deviation, z_c is the confidence coefficient for the 95% level ($z_c = 1.96$), and N is the number of samples in the distribution, less those discarded. The length of the uncertainty bars drawn vertically through each point in figure 9 is a representation of ΔV as computed by equation (1) for each data ensemble. That is, one can be 95% confident that the mean velocity, represented by the center of the square symbol in figure 9, lies somewhere along each uncertainty bar. Each velocity survey yields data similar to

those presented in figure 9 for the vertical and horizontal velocity components. A more visual representation of the data for the flow field is presented in figure 10, where velocity vectors have been drawn on the basis of the data shown in figure 9. Since the velocity vectors are based on the mean values for the velocity, the vectors represent a steady-state or time-averaged flow field. Some of the vector-direction scatter apparent in the velocity-vector plots shown in the figures can be attributed to variations caused by the atmospheric wind blowing past the doors in the building which houses the one-fiftieth-scale model and through which the jet blows. The doors had to be left open during the tests to allow discharge of the exhaust stream and thereby prevent induction of recirculating airflow.

TEST RESULTS

The deflector ramps listed in table 1 were evaluated by use of the one-fiftieth-scale model of the NFAC set up in the 80- by 120-Foot Wind Tunnel mode of operation. Each design was first evaluated by observing the yarn tufts, which indicated the magnitude and unsteadiness of the winds on the ground plane. One or more surveys were then made with the LV to obtain a quantitative measure of the velocity field induced by the exhaust jet. The results of these tests are summarized here by describing the response of the yarn tufts and presenting the velocity surveys downstream of the ramp. The first configuration studied consisted of the exhaust opening without a deflector ramp. The findings for the ramps listed in table 1 are then described. The objective is to find out how the ground winds are affected by the various characteristics of the deflector ramps.

Multiple surveys with the LV were first taken downstream of the exhaust opening when a ramp was not present (fig. 11). The expected spreading and deceleration of the jet (ref. 11) and the rounding of the velocity profile is apparent in the measurements, both in the side and top views of the flow field. The measured profiles also indicate that the flow in the lower part of the jet stays attached to the ground plane. As a consequence, the tufts under the jet moved actively, showing a highly unsteady movement of the air. Not indicated in figure 11, or in any of the velocity plots, is the turbulent or unsteady nature of the flow near the edges of the jet. The action of the tufts effectively monitors the variability of the flow with time, but it was not possible to depict this characteristic in a figure. These results suggest that the deflections of the elements of vane set #7, which is upstream of the screen and structural steel, were effective in turning most of the jet upward at about 40°, but lacked the control needed at the ground plane. The asymmetry of the exhaust opening (figs. 1, 2(b), and 7(b)) is no doubt responsible for the lack of symmetry in the velocity profiles shown in figure 11(b). As the jet proceeds downstream, it assumes a more rounded and symmetrical profile. The small reversed-flow regions on the lower part of figure 11(b) are attributed to the interference of atmospheric winds on the jet. This interference changes not only from day to day, but also during a test so that a number of idiosyncrasies in the velocity surveys appear which can be attributed to winds blowing past the doors of the building where the one-fiftieth-scale model is housed. Although the wind did

interfere somewhat with the tests, and did alter some of the velocity profiles
measured with the LV, the general conclusions regarding the effectiveness of the
ramp being studied was not affected. Although the wind did significantly affect the
smaller velocities around the jet edges, the data generally repeated quite well.
Variations in the wind did provide an opportunity to simulate the more realistic
conditions under which the full-scale facility is required to operate.

The closely spaced points in which data were taken for the multiple surveys
presented in figure 11 required about 10 hr of test time. It was therefore decided
to restrict the survey lines with the LV to only one line in the vertical direction
at a station located 0.91 m (36 in.) from the exhaust opening. It was found that
the qualitative observations of the yarn tufts, supported by the quantitative evalu-
ation of the velocity distributions at the one station, were sufficient to screen
the characteristics of the exhaust ramps. As a consequence, figures 12-19 present
velocity data at only the one survey station. The data are grouped in each of the
figures to show how the variation of a single parameter affects the velocity distri-
butions in the jet and those it induces near the ground.

One of the first observations made with the tufts was that the deflector ramps
should be placed next to the building directly on the ground plane. Since the
structure does not permit the lower part of the ramp to be located directly next to
the screen and vane set #7, it was always displaced slightly downstream, as indi-
cated in the figures. This displacement did not seem to affect the performance of
the ramps. However, a vertical displacement that left a small gap or slot between
the ground plane and the ramp did enhance the ground winds, as indicated by the
velocity surveys in figure 12. Therefore, all further tests were conducted with the
gap sealed by plastic tape.

Since the length and proper proportion of leakage and diversion were not known,
ramps of various lengths and porosity were tested at several angles relative to the
ground plane (figs. 13-16). Both the response of the yarn tufts and the character
of the velocity profiles at the 0.91-m (36-in.) station showed that a ramp with
about 30% porosity and 15.24 cm (6 in.) long at an angle of 45° provided the needed
effectiveness for the one-fiftieth-scale model. Larger (0.635-cm diam (0.25-in.),
more widely spaced holes (porosity = 23%) (fig. 16) were observed to be about as
good as the smaller or 0.32-cm-diam (0.125-in.) holes spaced for 30% porosity. As
anticipated, a solid ramp (i.e., no holes) caused a different kind of induced flow
at the ground plane (figs. 6 and 14) and was not as effective as those ramps with a
porosity between about 20% and 30%.

In all of the tests a measurable change was not detected in the pressures
inside the tunnel circuit or in the airspeed through the tunnel, even for the
25.4-cm (10-in.) ramp at 60° elevation angle. However, when the ramp was placed in
the vertical (i.e., at 90°), the tunnel test section lost about 10% in dynamic
pressure or about 5% in velocity whether or not the ramp was porous. The allevia-
tion of the winds (fig. 17) was observed from the tufts to be generally adequate,
with some disturbances to the tufts near the building, but quite adequate farther
away. This approach was not pursued further because of the unacceptably high loss

7

in tunnel performance even though the concept would be easy to implement by, for example, simply closing the lower one or two rows of doors in vane set #7.

A series of tests was then conducted to explore alternatives to flat ramps and uniform porosity in order to increase the possible materials and structural techniques that could be used to construct the full-scale deflectors. The curved ramps (fig. 18) were studied because they simulate many of the barriers used at airports to deflect the high-energy exhaust of the jet engines of aircraft upward and away from areas occupied by personnel or equipment which cannot tolerate the hot, high-velocity airstreams. The present application is very different from that at airports because of the ratio of the jet diameter to ramp length. In the wind tunnel situation, the jet thickness is over five times the height of the curved ramp used in the test (fig. 18). In the airport situation, the ramp size is usually two to four times the jet size. The test results show that the curved or circular shape in the wind tunnel application becomes a disadvantage (tufts and fig. 18) because the curved ramps are less effective than the flat ones.

Construction of a deflector ramp necessitates the use of support beams, corrugations, and other structural elements to obtain a structure that is both functional and strong enough to sustain the jet and atmospheric winds expected in a 40-yr lifetime. The support structure could be simplified if the porosity could be confined to strips on the ramp surface which are separated by nonporous strips. The relative widths of the strips are determined so that the average porosity is about 30%. For these reasons, tests were conducted on the last four configurations listed in table 1 (see fig. 19 for velocity profiles at 0.91 m station). Both the tuft motions and the velocity measurements indicate that the two configurations (figs. 19(b) and 19(d)) with the porosity confined to strips would be marginally satisfactory. They are not as effective as the plate with uniformly distributed 0.32-cm-diam (0.125-in.) holes. Materials with larger porosity such as the same ramps without the nonporous strips (figs. 19(a) and 19(c)) were found to be less effective than the 30% material.

On the basis of the results found for the tests on the deflector ramps listed in table 1, it was recommended that a ramp about 15.24 cm long (6 in. (or 25 ft full-scale)) with 0.32-cm (0.125-in.) holes uniformly distributed over the surface to produce a porosity of about 30% be scaled up and used for the full-scale application because it more than fulfills the objectives of the program. For this reason, more surveys were made with the LV to better define the velocity field of the jet and to be certain that any undesirable characteristic did not occur elsewhere in the flow field (fig. 20). The jet is noted to break cleanly from the ground plane and to remain detached thereafter. Both the yarn tufts and the velocity measurements indicate that the directly driven and the induced winds produced by the exhaust jet are of negligible intensity at the ground plane. Just as when a ramp was not present (fig. 11(b)) the jet has a slight asymmetry in the horizontal plane produced by differences in the building walls at the two sides of the jet. These idiosyncrasies are suppressed by turbulent mixing as the jet moves away from the exhaust opening.

The latitude in the design parameters is required to maintain sufficient effectiveness of the ramp, but is not a firm boundary. That is, if the ramp

performance is to be acceptable, deviations from the recommended design result in a slow degeneration of the performance. For example, a shortening of the already relatively small 15.24-cm (6-in.) ramp to, say, 12.7 cm (5 in.) for the model tunnel is probably acceptable, but further reductions are not, because conservatism is being lost. Enlargement of the ramp is usually not desired because of the added cost of construction, but any change above 15.24 cm (6 in.) would enhance the conservatism of the design. A change to smaller, more numerous holes while keeping the porosity fixed at about 30% is also acceptable, whereas use of holes larger than about 0.635 cm (0.25 in.) may be detrimental.

Toward the end of the experimental study, several end treatments were tried on the ramps. None of the end treatments seemed to affect the velocity distribution on the center plane of the jet. However, the induced velocities near the lower corners of the jet in the vicinity of the building were suppressed by end plates such as those presented in figure 21. Without end plates, the jet appears to draw in or ingest more air around the ends of the ramp than with the end plates. Hence, when end plates are present the jet separates more cleanly from the building and from the ground plane.

Photographs of smoke paths in and under the jet when a deflector ramp is not (fig. 22) and is (fig. 23) in place illustrate the change in the flow field brought about by the recommended ramp design. Without a ramp (fig. 22) the flow stays attached to the ground plane and is more turbulent (smoke path is more sinuous). When a ramp is in place, the smoke path indicates a clean separation from the ground (fig. 23). When smoke was placed under the jet, it remained relatively quiescent, rising slowly to join the flow along the lower part of the jet. The smoke essentially confirms the results observed with yarn tufts and with the LV.

APPLICATION TO FULL-SCALE FACILITY

The experimental data on deflector ramps described in the previous section were all obtained with a one-fiftieth-scale model of the NFAC. Decisions now need to be made on how to scale and adapt these small-scale results to effectively apply them to the full-scale facility. If all dimensions are increased by a factor of 50, the ramp becomes 7.62 m (25 ft) long and the holes become 15.24 cm (6 in.) in diameter. Since it is easier to obtain materials with smaller holes, and the smaller holes were predicted to sustain effectiveness, the porosity will probably be achieved with sheet metal having a uniform distribution of holes about 2.5 cm (1 in.) in diameter. The support structure for the porous plate will need to fit under and around the superstructure on the outside of the building (figs. 2(b) and 4). Several possible adaptations that are acceptable are presented in figure 24. The design which minimizes the amount of interference between existing and new structures, and which is lowest in cost, is the one that will probably be chosen (fig. 24(c)).

9

Another concern that arises in the full-scale use of the 80- by 120-Foot Wind Tunnel is the persistence of the jet to altitudes occasionally used by aircraft. Whether the wind shear and jet velocities really do pose a hazard to low-flying aircraft was investigated by first developing empirical relationships for the jet-velocity distribution. These relationships are needed to extend the data to distances beyond those measured with the one-fiftieth-scale model. Since a high degree of precision is not needed, the approximations of a self-similar model for turbulent circular jets (Chapter XXIV of Schlichting, ref. 12) was chosen as the basis for the extrapolation. Application will be made only to the jet structure when a deflector ramp is present for which data are available (fig. 20). The width or depth of the jet is taken as proportional to the distance, $(x - x_v)$, from a virtual origin; and the centerline velocity, U_{l_c}, as inversely proportional to $(x - x_v)$. Based on the data in figure 20, the virtual origin which best fits the velocity distribution is located 183 cm (72 in.) upstream from the exhaust opening of the model. At full scale, the virtual origin is 50 times as far, or $x_v = -91.3$ m (-300 ft). The equations for the velocity on the centerline of the jet are then given by

$$U_{l_c} = \frac{192}{x + 72} \times 26 \text{ knots} \tag{2a}$$

for the model tunnel at its operating speed (x is in inches from the exhaust opening); and

$$U_{l_c} = \frac{800}{x + 300} \times 48.5 \text{ knots} \tag{2b}$$

for the full-scale tunnel at its maximum operating speed (x is in feet) of 100 knots in the test section. The data in figure 20 are compared with the foregoing relationship in figure 25. The quantity x is the horizontal distance from the exhaust opening and not the distance along the jet. Since the jet is inclined at roughly 38° from the horizontal, the two lengths are related by the cosine of 38°.

Since the exhaust opening is rectangular in shape and not round, the jet spreading with horizontal distance is different for the width and for the depth of the jet. The same virtual origin does not apply for depth and breadth because two size relationships are needed. The data for the model and their linear approximations are presented in figure 26. It is to be noted that the jet spreads such that the difference between the magnitude of the width and depth remains approximately constant.

The data presented herein and represented by the foregoing equations were obtained in essentially still air. Even though wind was present on occasion, an

10

effort was made to minimize its net effect and any bias it might put in the data. Under actual full-scale operation, atmospheric winds will often be blowing hard enough to alter the velocity and shape of the jet, especially at the larger distances from the exhaust opening. A limit on this interference is set by the criterion that the 80 by 120 does not operate if the wind magnitude is greater than 20 knots.

With the foregoing relationships for the structure of the jet, a simulation was carried out by Streeter (ref. 12) of the interaction of an aircraft with the jet as it penetrates the plume from different directions and altitudes. In summary of reference 12, it was learned that an aircraft at higher altitudes will be affected a negligible amount by the jet disturbance. However, as the altitude of penetration decreases, the jet velocity increases to such an extent that considerable perturbations of the flightpath is experienced. Reference 12 presents details of the aircraft/jet interaction.

CONCLUDING REMARKS

The exhaust plume of the 80- by 120-Foot Wind Tunnel as it leaves the facility was found to cause intolerably high winds on the ground and around other buildings in the vicinity of the jet. The experimental program described here identified the characteristics of a deflector ramp that would reduce the magnitude of the undesirable winds to a negligible level. Since the parameters that govern the ramp design are effective over a range of values, some latitude is available for implementation of the full-scale ramp. Based on the test results obtained with the one-fiftieth-scale model of the tunnel, the full-scale deflector ramp should be placed on the ground next to the exhaust opening. It should have a slant length of about 7.62 m (25 ft) or more, and should be elevated at an angle of about 45° to the ground plane. The surface material should preferably have a porosity of about 30%, which is produced by uniformly distributed holes 15.24 cm (6 in.) or less in diameter. The east and west ends of the ramp should be capped with plates to suppress unwanted eddies.

11

REFERENCES

1. Eckert, William T.; Mort, Kenneth W.; and Piazza, J. E.: Wind-Sensitivity Studies of a Non-Return Wind Tunnel With a 216- by 432-mm (8.5- by 17.0-in.) Test Section - Phase I. NASA TM X-62,171, 1972.

2. Eckert, William T.; Mort, Kenneth W.; and Piazza, J. E.: Wind Sensitivity Studies of a Non-Return Wind Tunnel, With a 216- by 432-mm (8.5- by 17.0-in.) Test Section - Phase II. NASA TM X-62,307, 1973.

3. Mort, K. W.; Eckert, W. T.; and Kelly, M. W.: The Steady-State Flow Quality of an Open Return Wind Tunnel Model. Canadian Aeronautics and Space Journal, vol. 18, no. 9, Nov. 1972, pp. 285-289. (See also NASA TM X-62,170, 1972.)

4. Mort, Kenneth W.; Soderman, Paul T.; and Eckert, William T.: Improving Large-Scale Testing Capability by Modifying the 40- by 80-Ft Wind Tunnel. AIAA Journal of Aircraft, vol. 16, no. 8, Aug. 1979, pp. 571-575.

5. Eckert, William T.; and Mort, Kenneth W.: Wind vs. Wind Tunnel: The Aerodynamics of the Inlet for NASA's New Very Large, Non-Return-Flow Facility. Journal of Wind Engineering and Industrial Aerodynamics, vol. 9, no. 3, Mar. 1982, pp. 193-205.

6. Mort, K. W.; Engelbert, D. F.; and Dusterberry, J. C.: Status and Capabilities of the National Full Scale Facility. AIAA Paper 82-0607, Mar. 1982.

7. Corsiglia, Victor R.; Olson, Lawrence E.; and Falarski, Michael D.: Aerodynamic Characteristics of the 40- by 80-/80- by 120-Foot Wind Tunnel at NASA Ames Research Center. AIAA Paper 84-0601, Mar. 1984.

8. Dudley, M. R.; Unnever, G.; and Regan, D. R.: Two-Dimensional Wake Characteristics of Inlet Vanes for Open-Circuit Wind Tunnels. AIAA Paper 84-0604, Mar. 1984.

9. Reinath, M. S.: Laser Velocimeter for Large Wind Tunnels. AIAA J. of Aircraft, vol. 19, no. 12, Dec. 1982, pp. 1100-1102.

10. Reinath, M. S.; Orloff, K. L.; and Snyder, P. K.: A Laser Velocimeter System for the Ames 40- by 80-Foot and 80- by 120-Foot Wind Tunnels. AIAA Paper 84-0414, Jan. 1984. (See also NASA TM 84393.)

11. Schlichting, Hermann: Boundary-Layer Theory. McGraw-Hill Book Company, New York, 1979.

12. Streeter, Barry G.: Simulator Investigation of the Effect of the Ames 80' by 120' Wind Tunnel Exhaust Flow on Light Aircraft Operating in the Moffett Field Traffic Pattern. NASA TM 86819, 1985.

TABLE 1.- FLOW DEFLECTORS TESTED WITH ONE-FIFTIETH-SCALE MODEL OF
80- BY 120-FOOT WIND TUNNEL

Material	Cross-sectional shape	Length of ramp surface, cm (in.)	Angle of inclination, deg	Figure number where velocity is shown
None	---	---	---	9, 10, 11
Solid plate; 0% porosity	Flat	6.1 (2.4)	45	14a
		12.7 (5)	45	12, 14b
		15.24 (6)	90	17a
		25.4 (10)	45	14c
	Circular arc	12.7 (5)	45	18a
Porous plate, 0.32-cm (1/8-in.) holes; 30% porosity	Circular arc	12.7 (5)	45	18b
	Flat	10.2 (4)	45	15a
		12.7 (5)	45	15b
		15.24 (6)	45	15c, 20, 25
		15.24 (6)	90	17b
		25.4 (10)	30, 45, 60	13
Porous plate, 0.635-cm (1/4-in.) holes; 23% porosity	Flat	10.2, 15.24 (4,6)	45	16
Wire screen, 43% porosity	Flat	15.24 (6)	45	19c
With taped strips	Flat	15.24 (6)	45	19d
Expanded metal mesh, 75% porosity	Flat	15.24 (6)	45	19a
With taped strips	Flat	15.24 (6)	45	19b

13
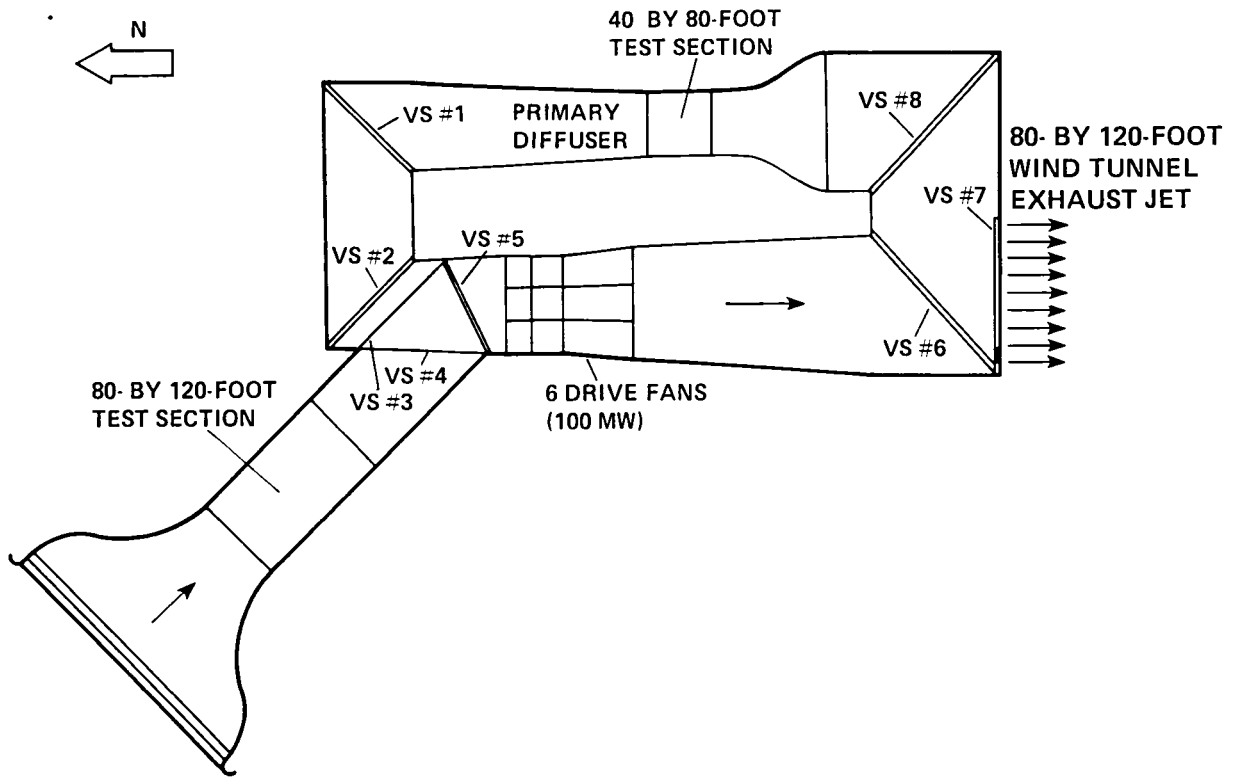
Figure 1.- Diagram of plan view of the National Full-Scale Aerodynamics Complex at
NASA Ames Research Center which illustrates 40- by 80-Foot and 80- by 120-Foot
Wind Tunnel circuits.
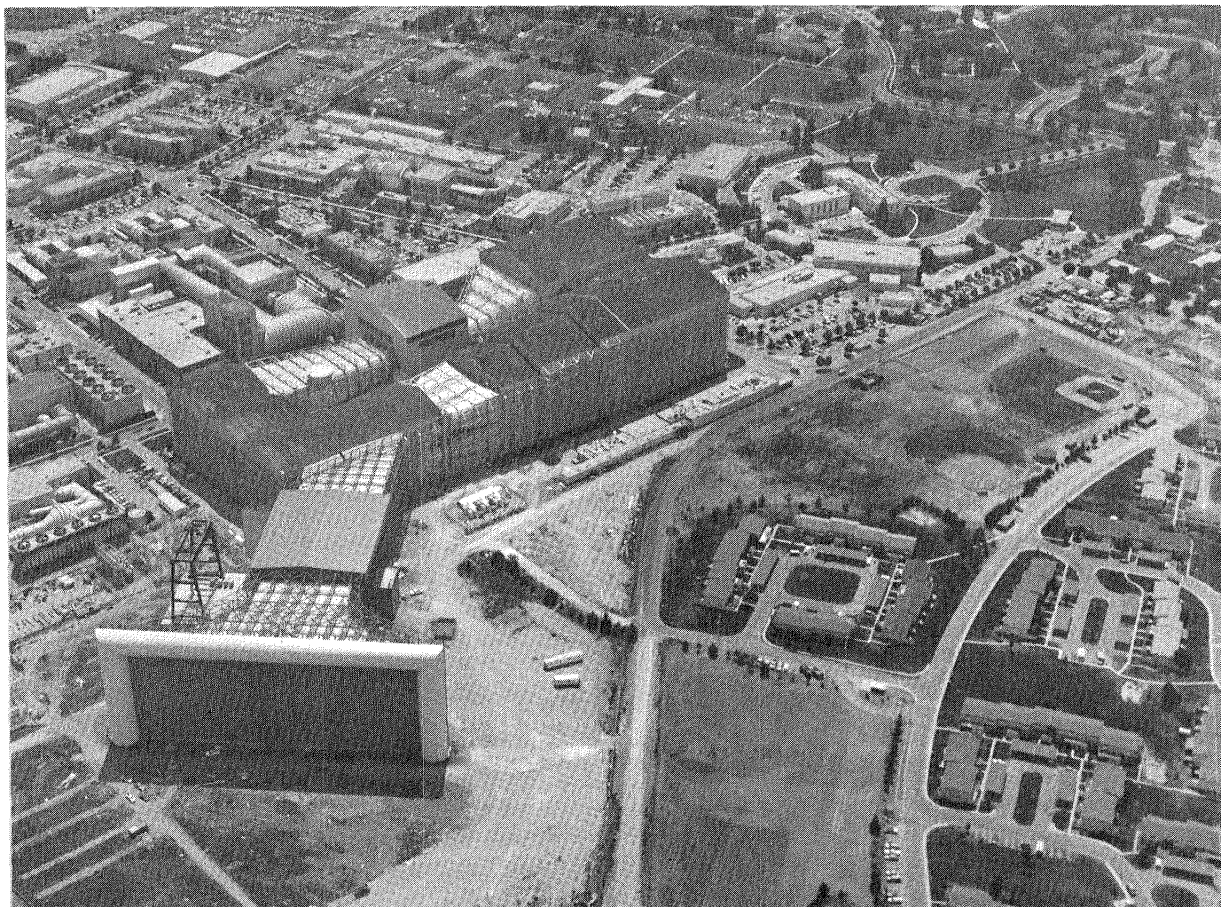
(a) View of facility looking into the entrance of 80- by 120-Foot Wind Tunnel
from the northwest. (AC 82-0551-54)

Figure 2.- National Full-Scale Aerodynamics Complex showing the entrance and
exhaust of the 80- by 120-Foot Wind Tunnel and the surrounding buildings.
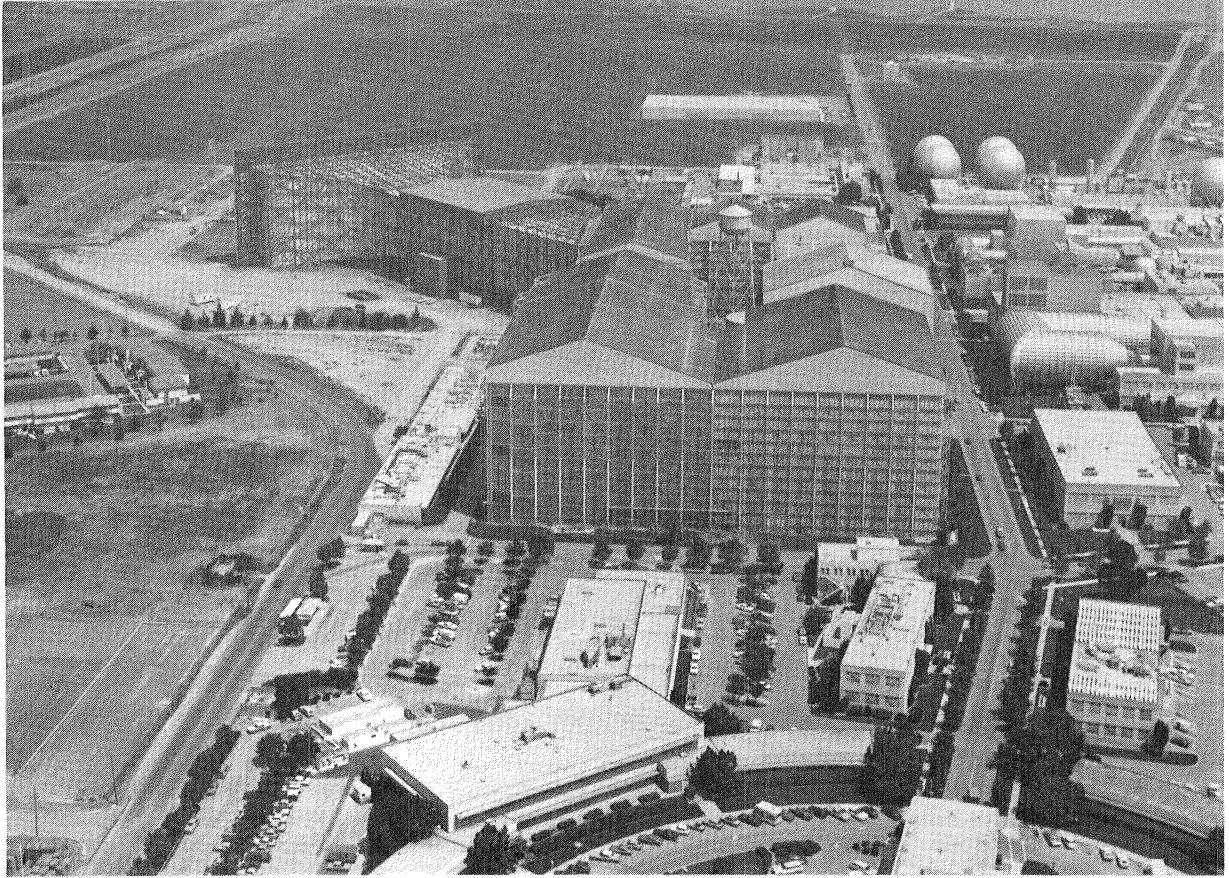
(b) View of NFAC looking into exhaust opening from the south. (AC 82-0551-43)

Figure 2.- Concluded.
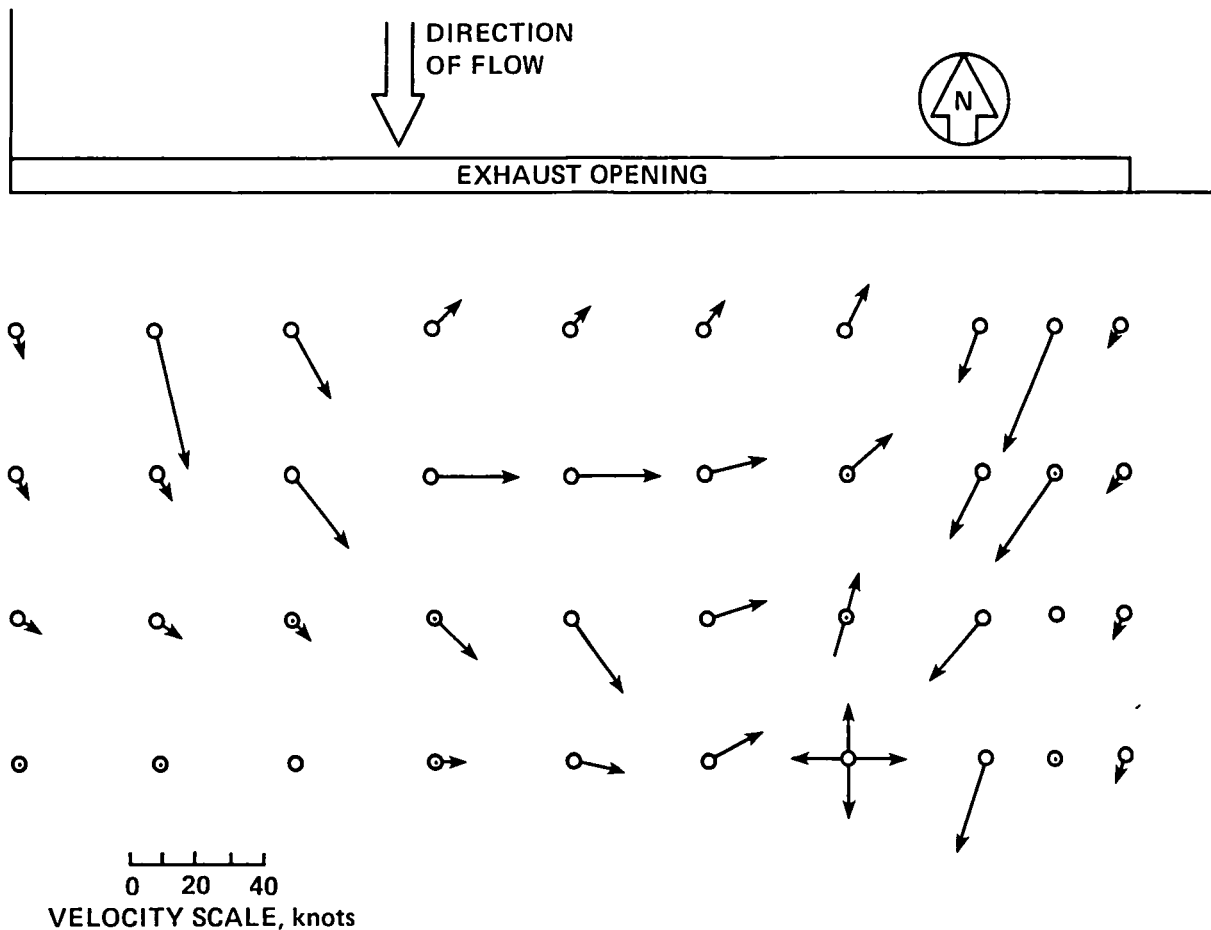
Figure 3.- Plan view of wind vectors measured with a hand-held wind anemometer on the ground under the exhaust jet during the 1982 tests of the full-scale facility. (Run 12, fan drive blade angle = 44°, 12-9-82); $V_{test\ section} \approx 86$ knots, $V_{jet\ b} \approx 40$ knots, P = 77.7 MW.
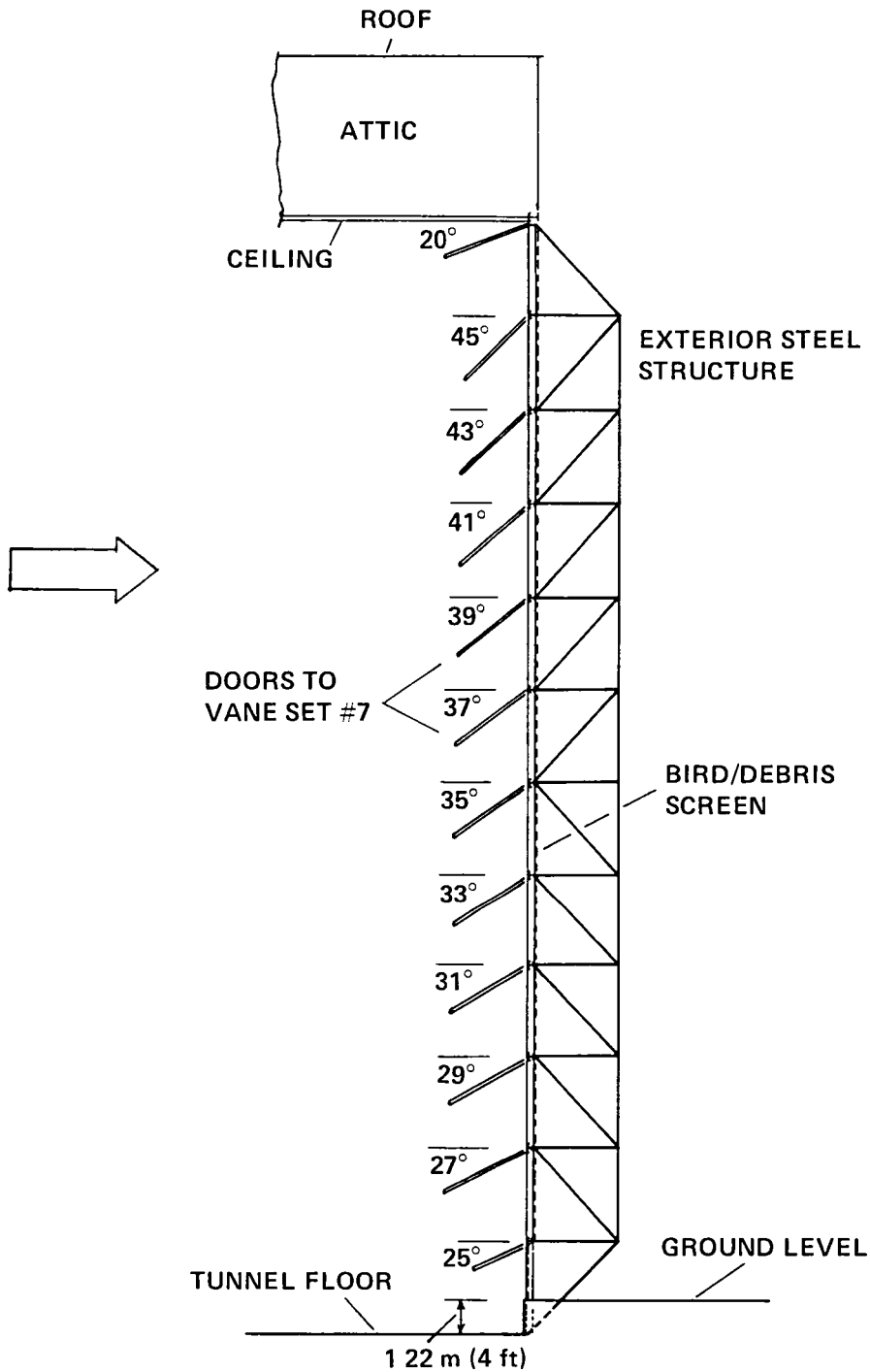
Figure 4.- Side view of cross section of vane set #7 and exhaust opening which illustrates splay angles of doors and offset of tunnel floor from ground level.

COURTYARD OF
40- BY 80-FOOT
WIND TUNNEL
CIRCUIT

POSITION OF FLAPS FOR
OPERATION OF 40- BY
80-FOOT WIND TUNNEL

VS #6

POSITION OF FLAPS FOR
OPERATION OF 80- BY
120-FOOT WIND TUNNEL

WEST
WALL

VS #7 IN OPEN
POSITION
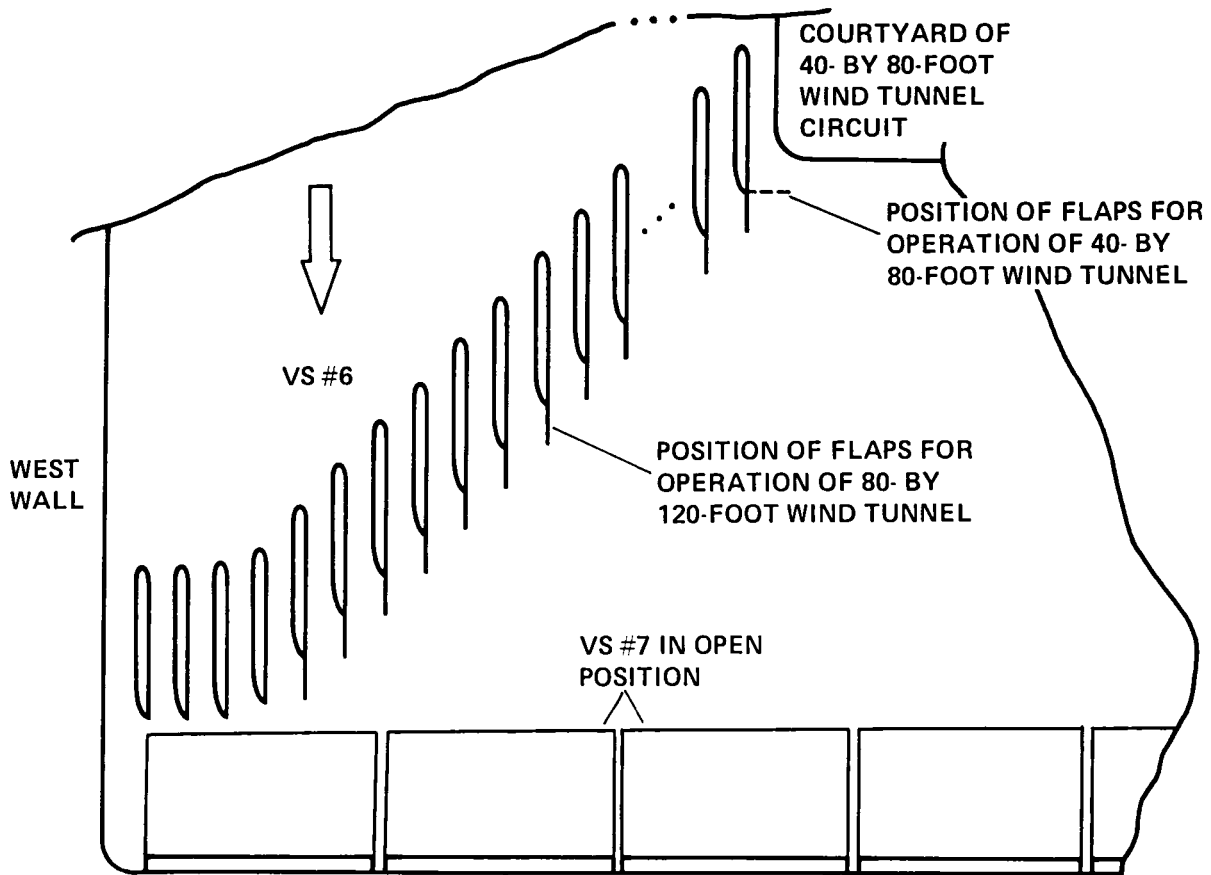
Figure 5.- Plan view of southwest corner of NFAC which illustrates offset of three corner vanes and removal of four flaps from VS #6 (which contains a total of 57 vanes) to accommodate the inward swing of VS #7 as it opens for 80- by 120-Foot Wind Tunnel operation. Debris screen and structure on outside of building are not shown.

19
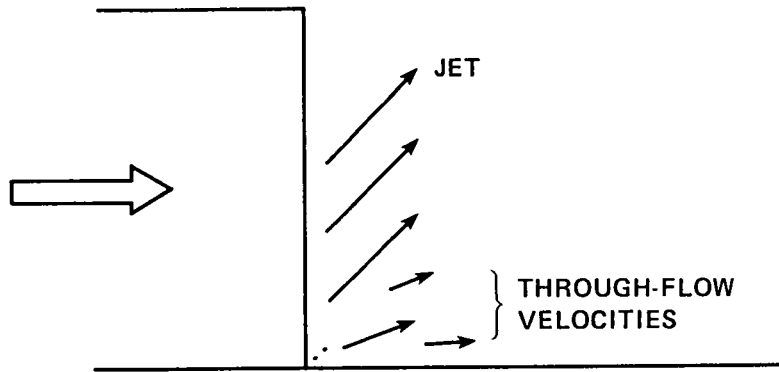
(a) Flow field when ramp is too porous or nonexistent.
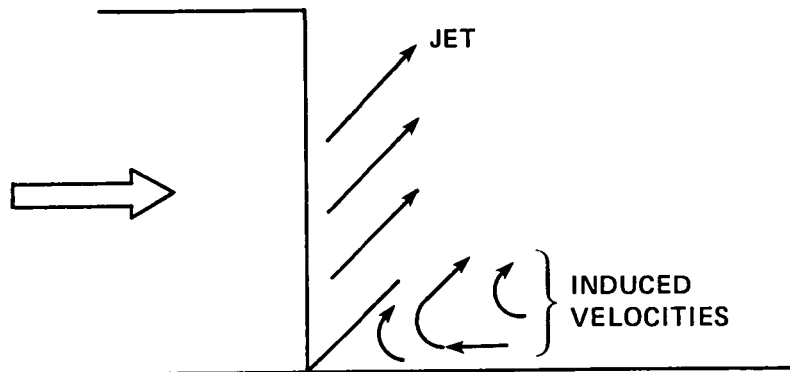
(b) Flow field when ramp is solid or nonporous.
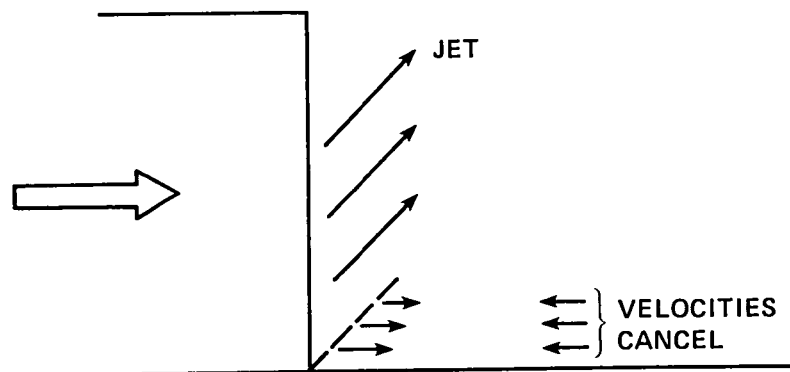
(c) Induced velocities at ground are negligible when size and porosity of ramp are correctly chosen so that induced and through-flow velocities cancel one another.

Figure 6.- Schematic side view of exhaust jet and opening with a ramp to illustrate concept on which design of porous ramp is based.
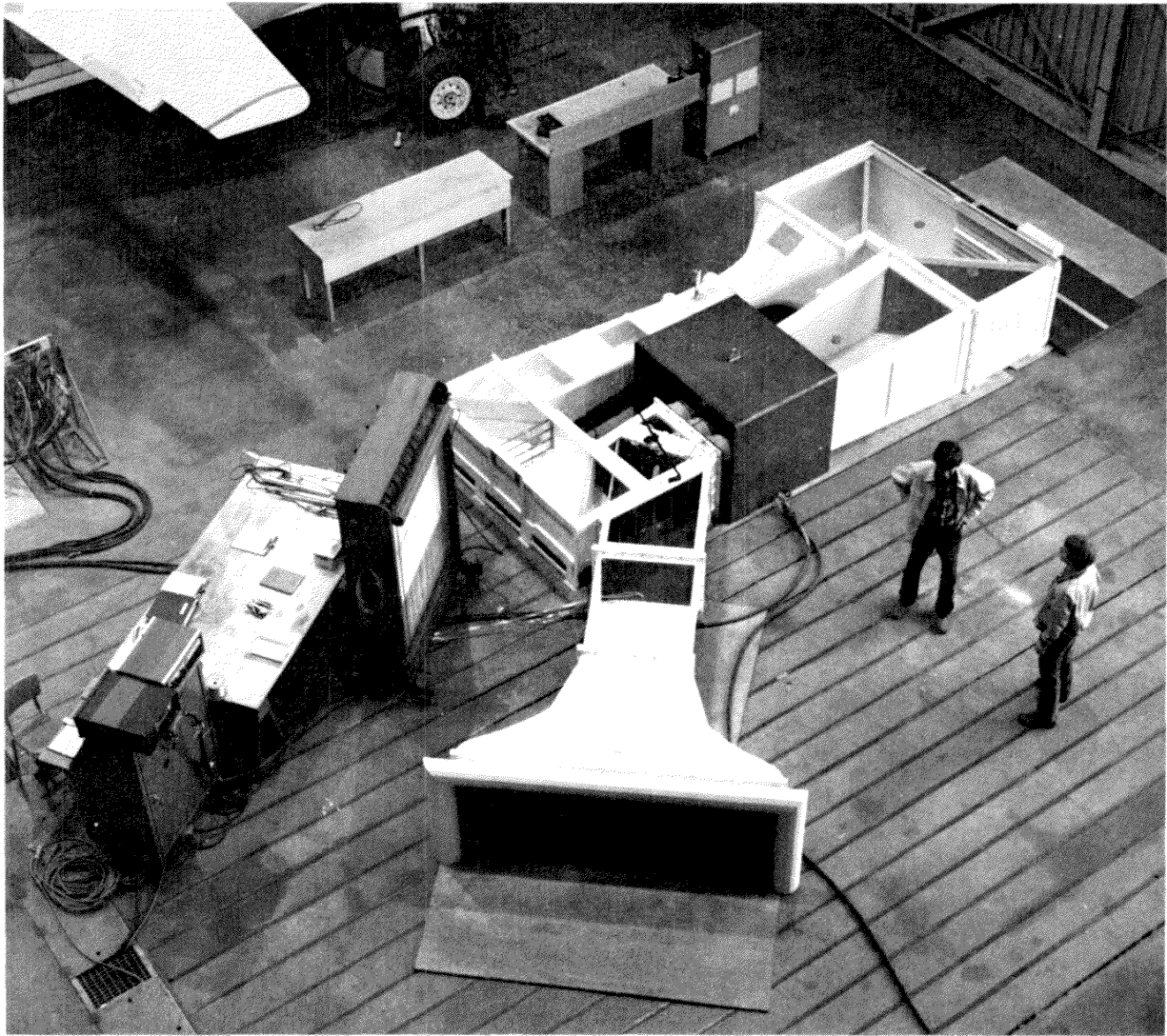
(a) Overhead view looking along entry and test section parts of 80- by 120-ft circuit.   (AC 83-8003-10)

Figure 7.- One-fiftieth-scale model of NFAC used in the experimental investigation.
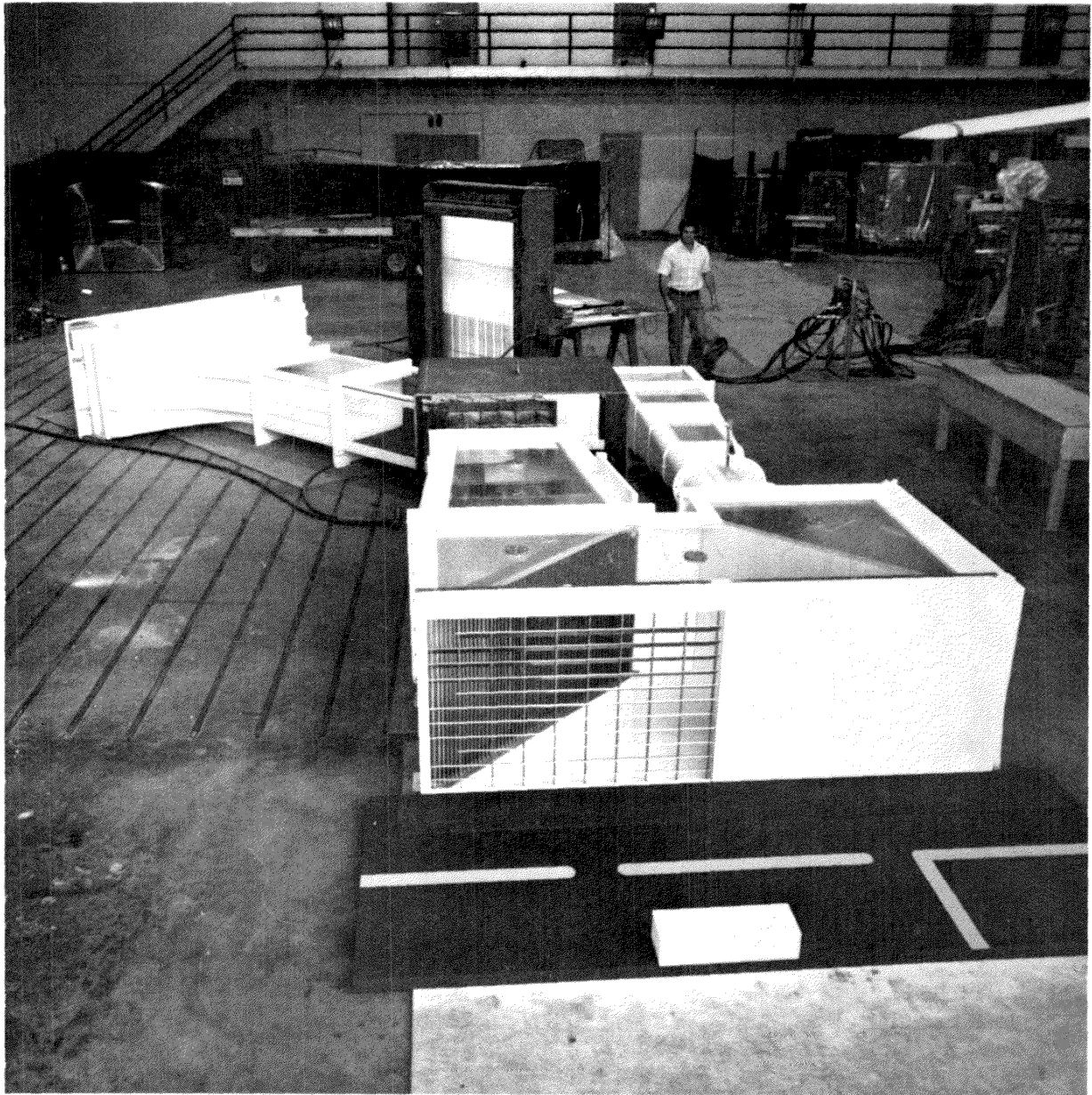
(b) View looking at south end of NFAC with VS #7 in open position.   (AC 83-8003-18)

Figure 7.- Concluded.
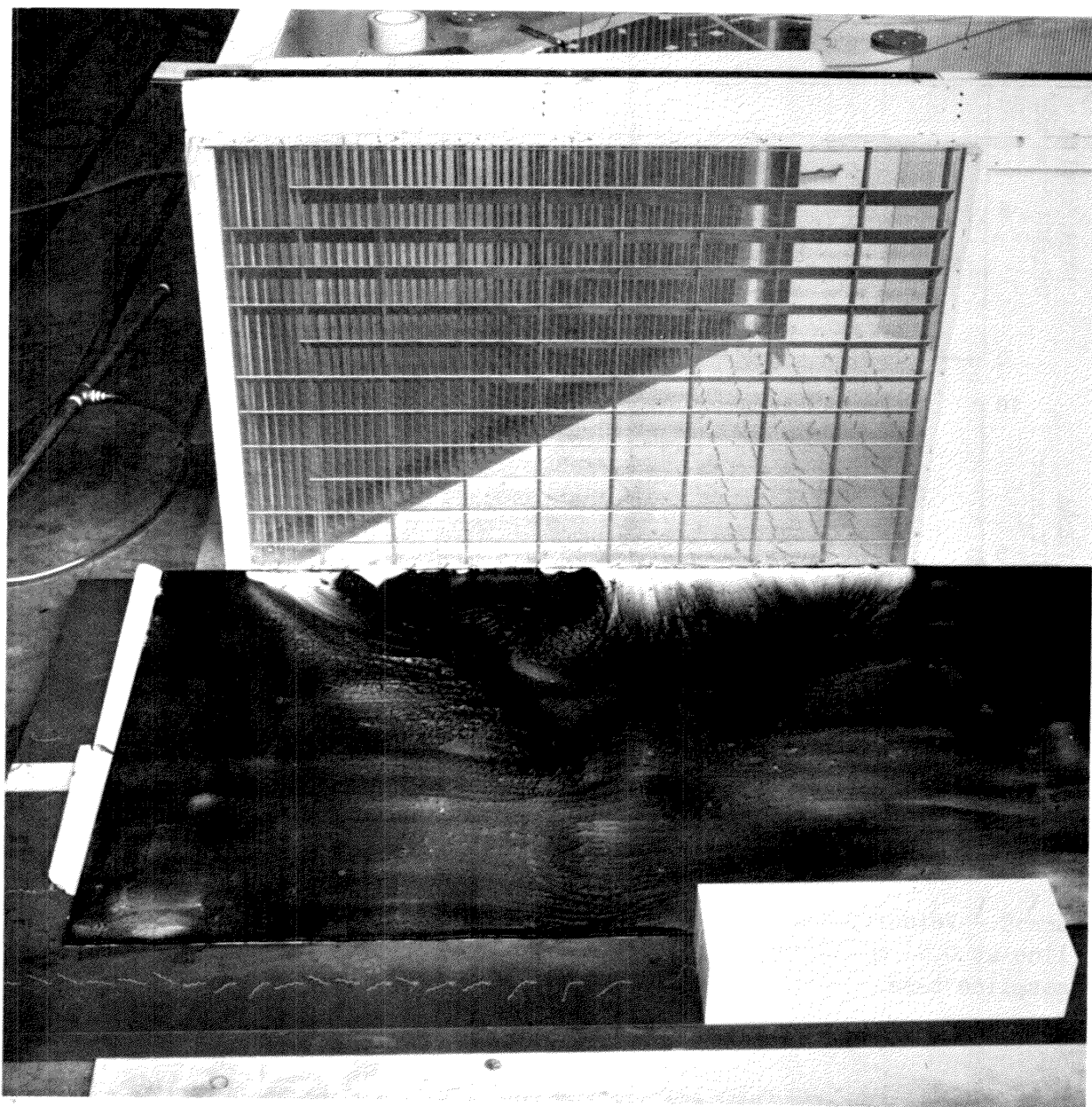
Figure 8.- Streaks scrubbed in an oil smear by winds on ground plane under exhaust
jet of one-fiftieth-scale model. Note similarity with velocity vector pattern
measured full scale and presented in figure 3. (A83-8003-19)
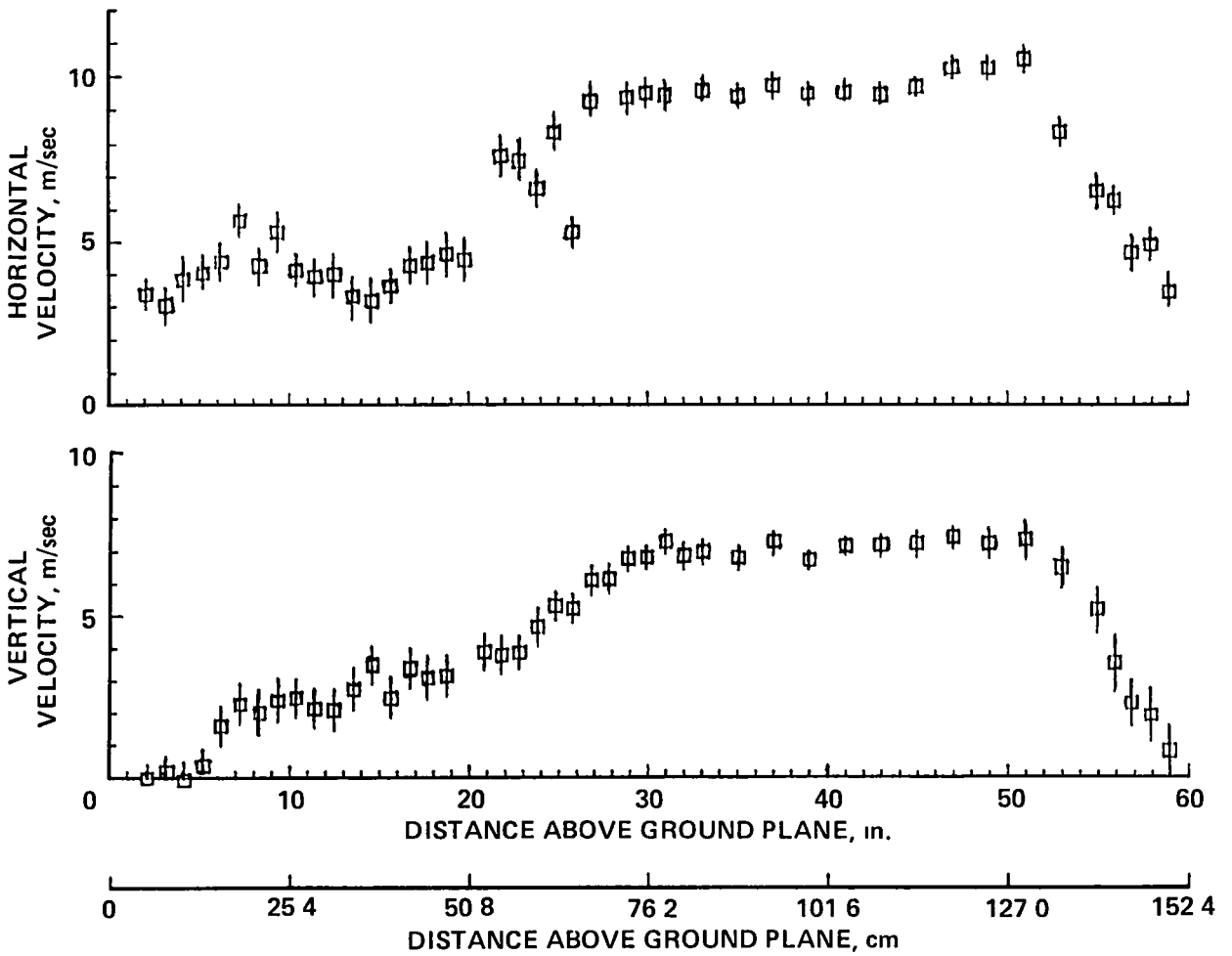
Figure 9.- Velocity data taken with LV along a vertical line located on jet center-line at 0.91 m (36 in.) from exhaust opening. No ramp in flow field which is baseline case.
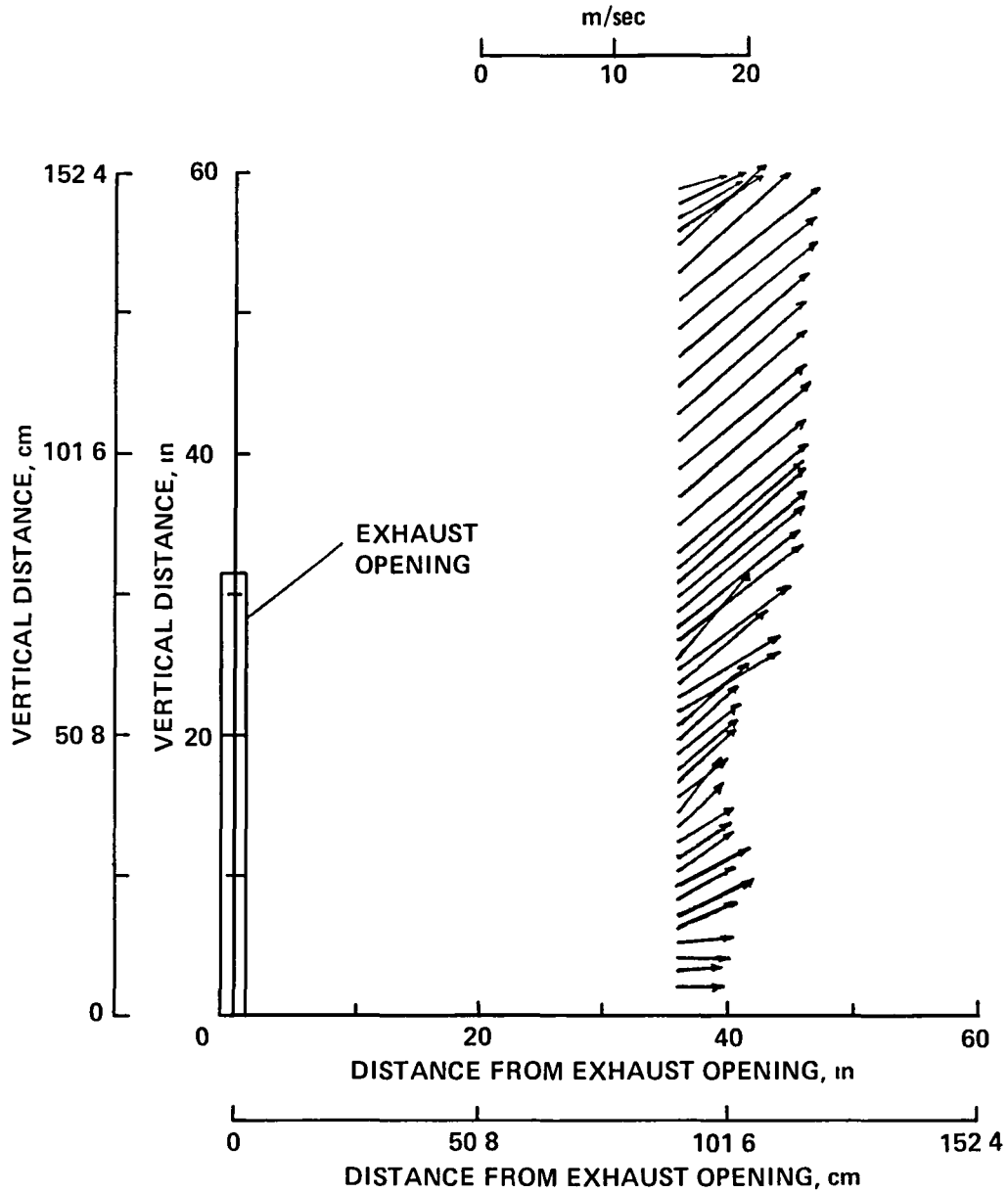
Figure 10.- Vector representation of data presented in figure 9 for the velocity distribution along a vertical line located on jet centerline at 0.91 m (36 in.) from exhaust opening. No ramp in flow field which is baseline case.
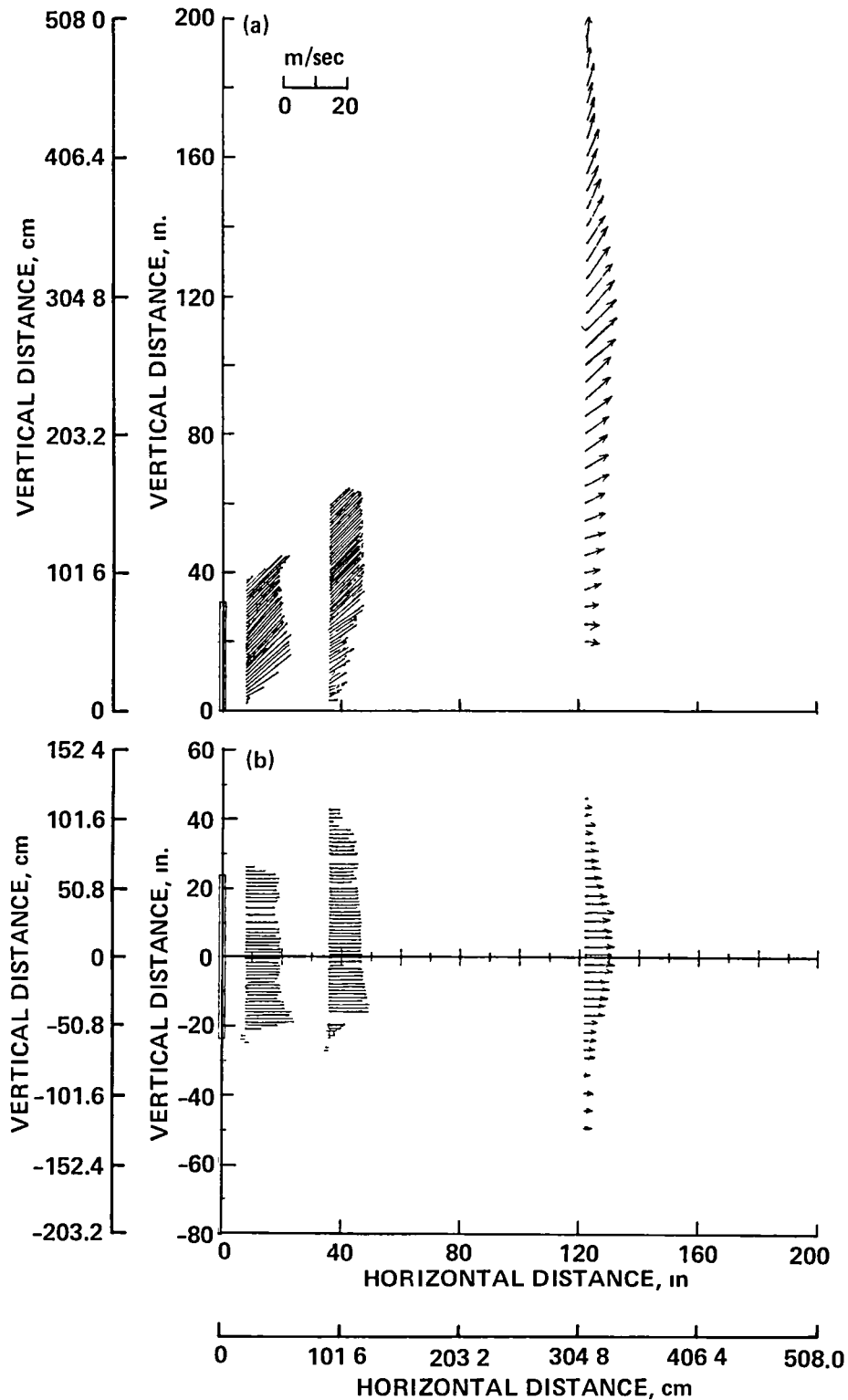
Figure 11.- Vector representation of velocity in flow field downstream of exhaust opening without deflector ramp as constructed for 1982 IST (baseline case); V_{ts} = 55 knots (28 m/sec). (a) Side view of velocity distributions along vertical traverses through centerplane of jet. (b) Top view of velocity distribution along horizontal traverses through center of jet.
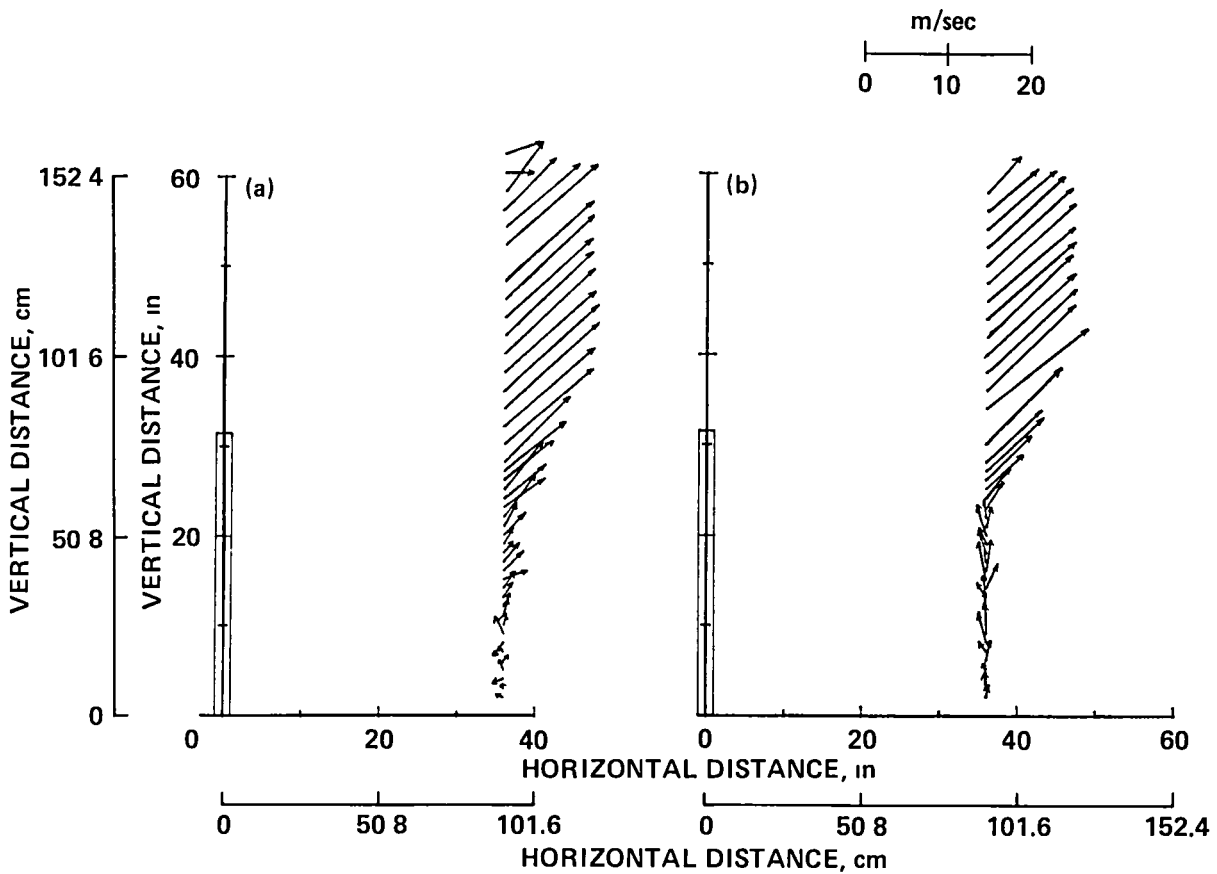
Figure 12.- Vector representation of velocity surveys taken along a vertical traverse 0.91 m (36 in.) from exhaust opening when a 12.7-cm (5-in.) ramp with no porosity and elevated at 45° to the ground plane is present next to the lower end of the exhaust opening. V_{ts} = 55 knots. (a) Gap exists between ground plane and ramp. (b) Gap sealed with plastic tape.
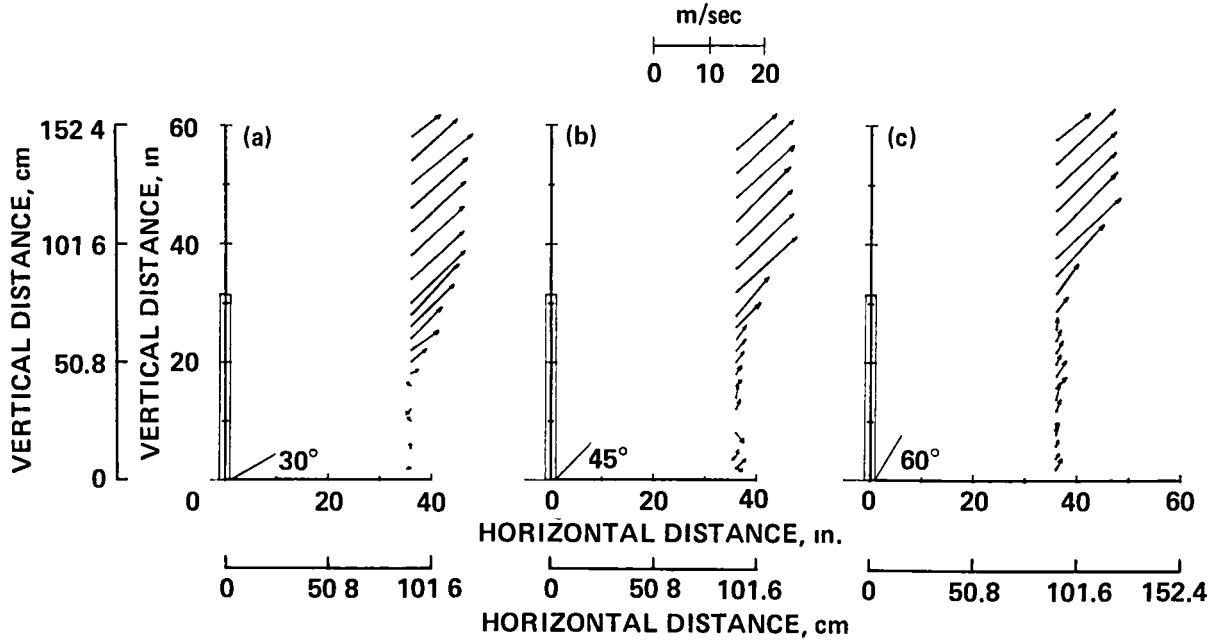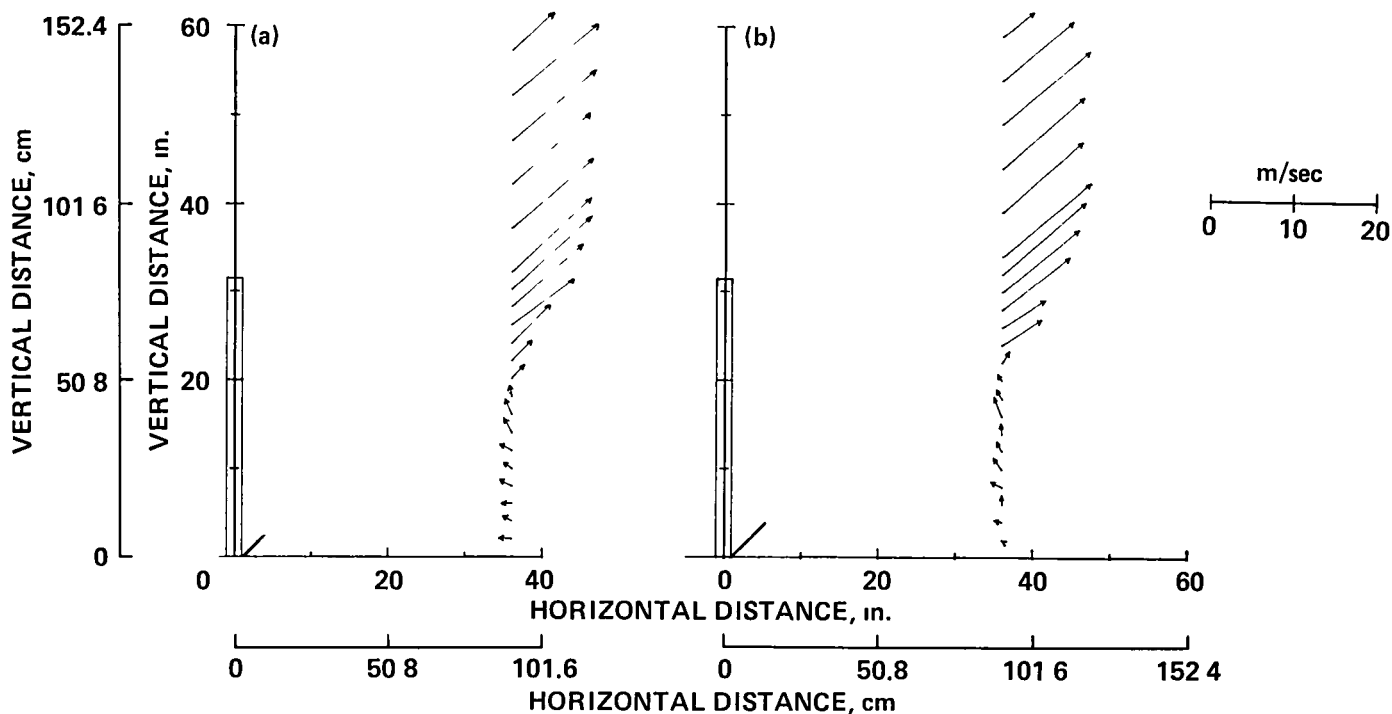
Figure 13.- Vector representation of velocity distribution taken along vertical
traverse at 0.91 m (36 in.) from exhaust opening with 25.4-cm (10-in.) ramp
0.32 cm (0.125 in.) holes; porosity = 30%. (a) Ramp angle = 30°. (b) Ramp
angle = 45°. (c) Ramp angle = 60°.
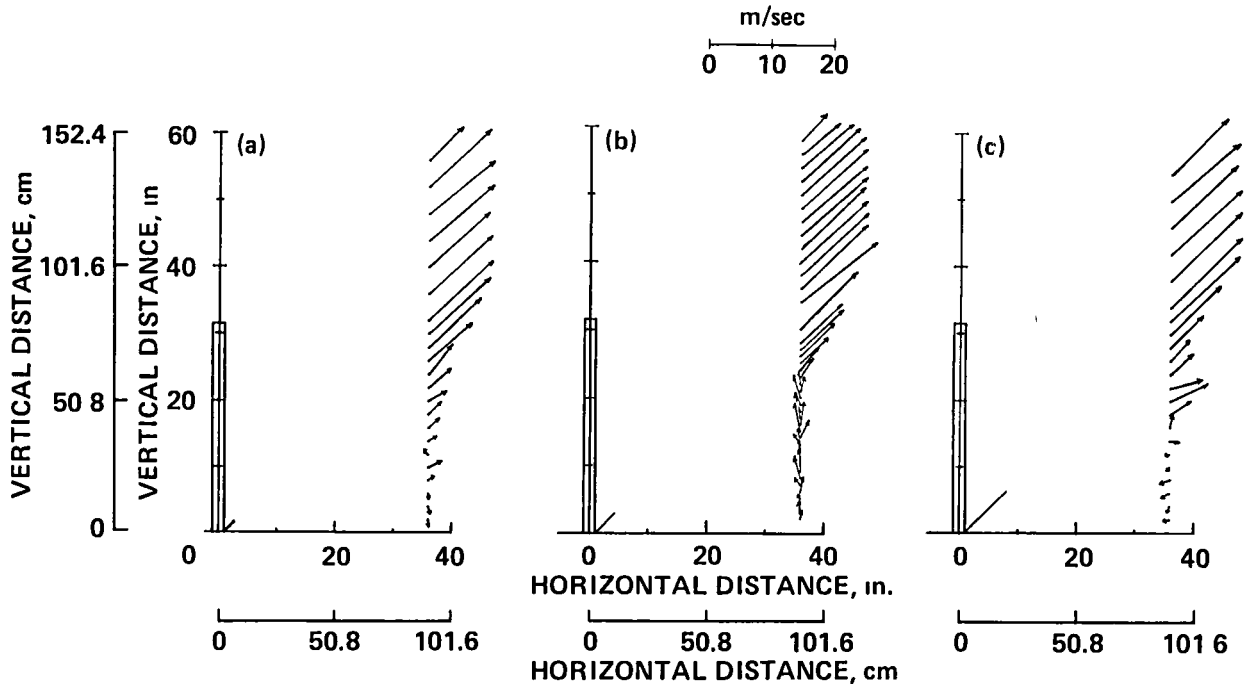
Figure 14.- Vector representation of velocity distribution taken along vertical
traverse at 0.91 m (36 in.) from exhaust opening when solid ramps (0% porosity)
of different lengths are used to deflect the jet. (a) Ramp length = 6.1 cm
(2.4 in.). (b) Ramp length = 12.7 cm (5 in.). (c) Ramp length = 25.4 cm
(10 in.).
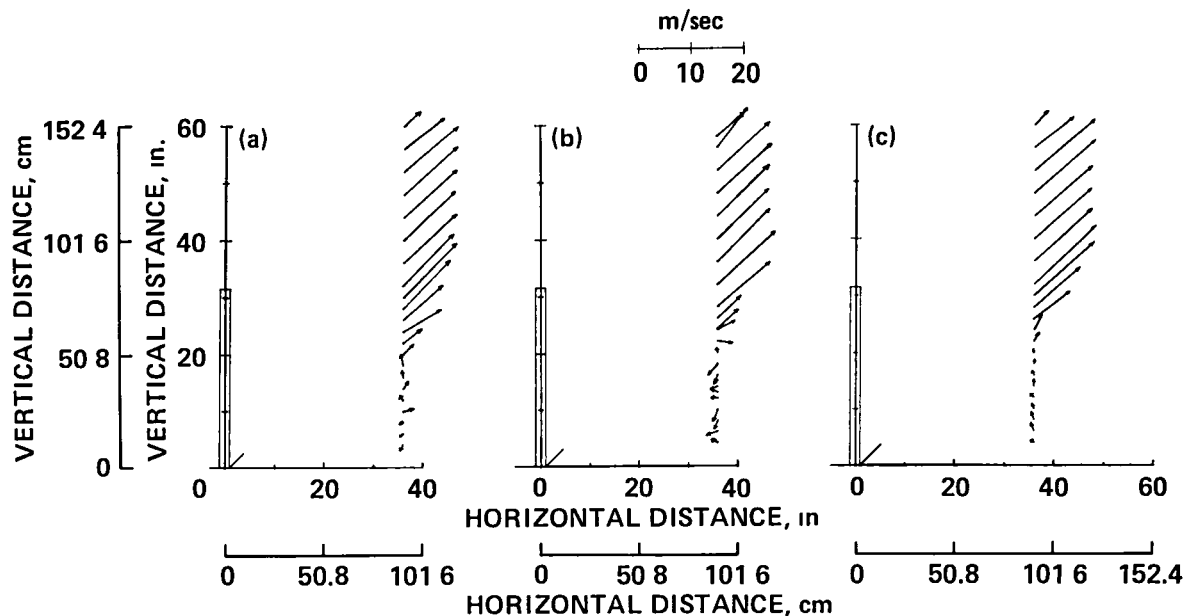
Figure 15.- Vector representation of velocity distribution taken along vertical traverse at 0.91 m (36 in.) from exhaust opening when porous 0.32-cm (0.125-in.) holes; 30% porosity ramps at 45°, but with different lengths are used to deflect the jet. (a) Ramp length = 10.2 cm (4 in.). (b) Ramp length = 12.7 cm (5 in.). (c) Ramp length = 15.24 cm (6 in.).
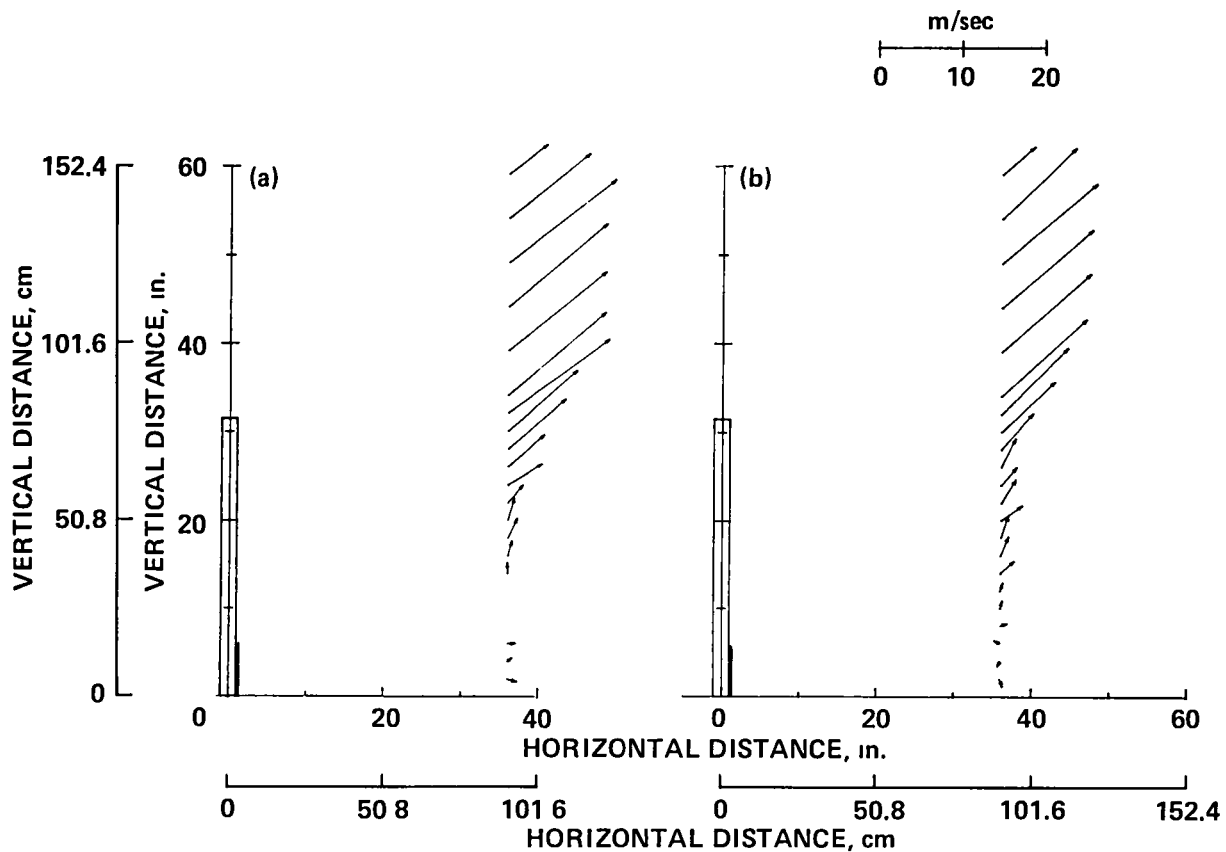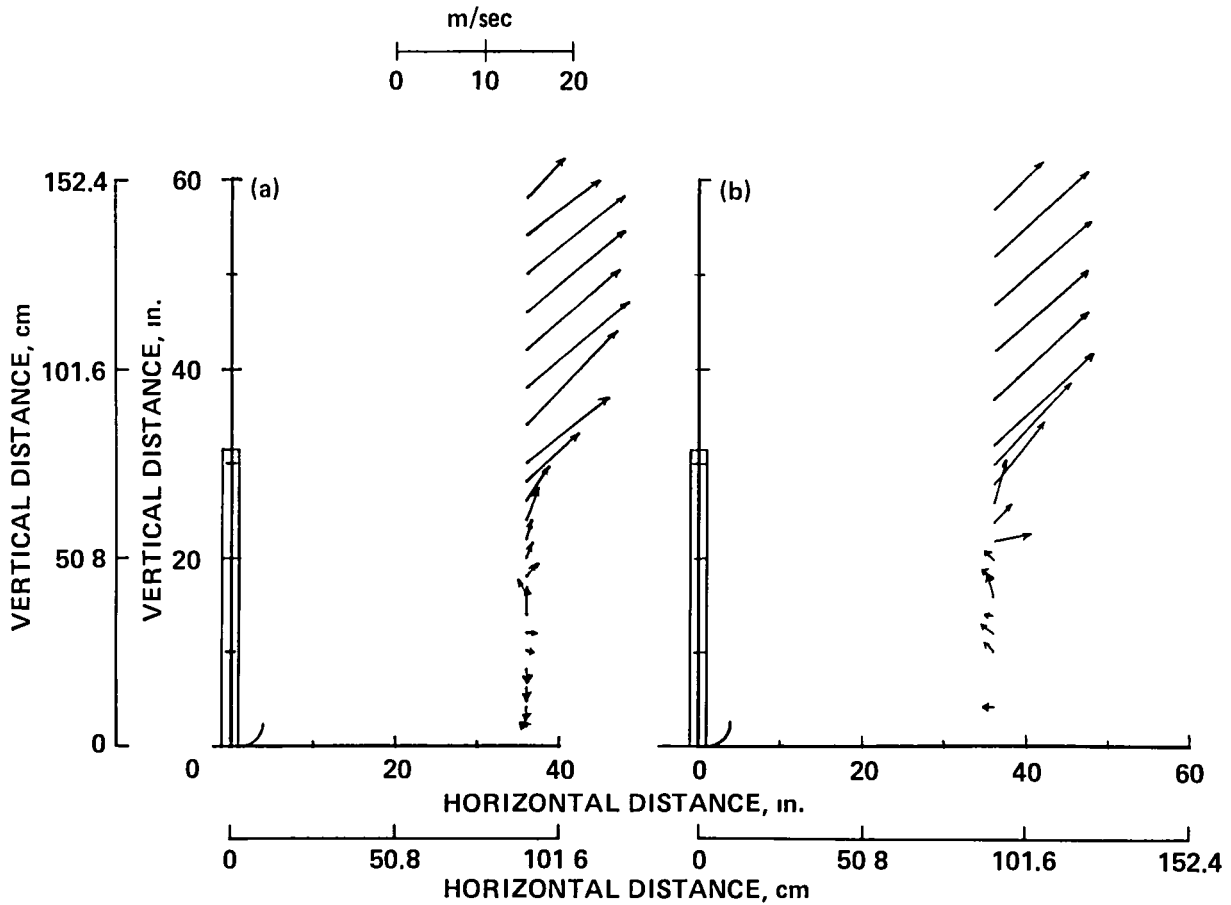

Figure 16.- Vector representation of velocity distribution taken along vertical traverse at 0.91 m (36 in.) from exhaust opening when porous 0.635 cm (0.25 in.) holes; 23% porosity, ramps at 45°, but with different lengths are used to deflect the jet. (a) Ramp length = 10.2 cm (4 in.). (b) Ramp length = 15.24 cm (6 in.).
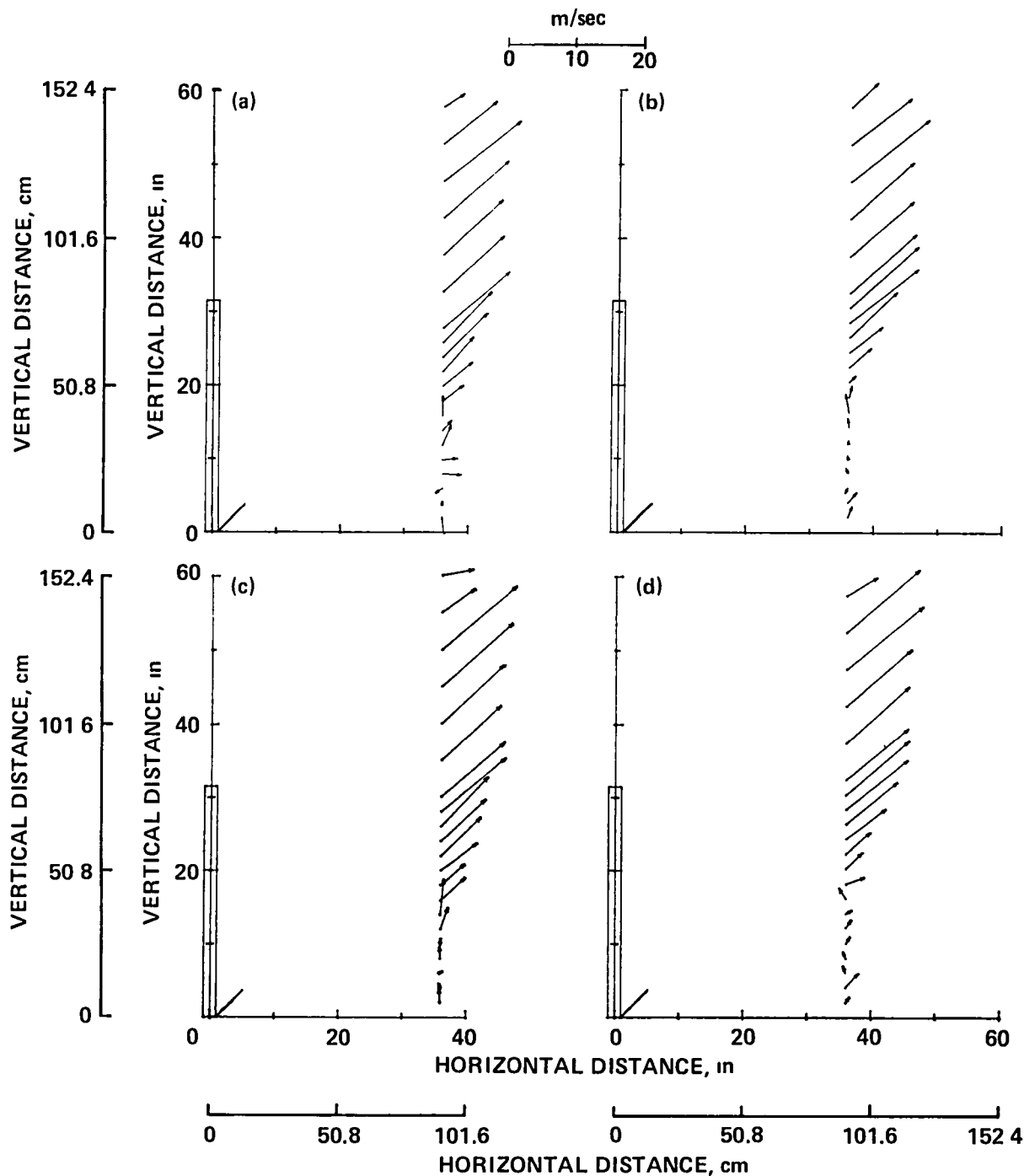
29

Figure 17.- Vector representation of velocity distribution taken along vertical traverse at 0.91 m (36 in.) from exhaust opening when ramps 15.24 cm (6 in.) long at 90° but of different porosity are placed along lower edge of opening. (a) Solid or 0% porosity. (b) 0.32 cm (0.125 in.) holes for 30% porosity.

Figure 18.- Vector representation of velocity distribution taken along vertical traverse at 0.91 m (36 in.) from exhaust opening when ramps with circular arc curvature 12.7 cm (5 in.) long but with different porosity are used to deflect jet. (a) Solid or 0% porosity. (b) 0.32 cm (0.125 in.) holes for 30% porosity.

Figure 19.- Vector representation of velocity distribution taken along vertical
traverse at 0.91 m (36 in.) from exhaust opening when ramps 15.24 cm (6 in.) long
with nonuniform porosity at 45° are used. (a) Expanded metal mesh
(porosity = 75%). (b) Expanded metal mesh (porosity = 75%) with taped strips
0.953 cm (3/8 in.) wide spaced 0.635 cm (1/4 in.) apart to yield an average
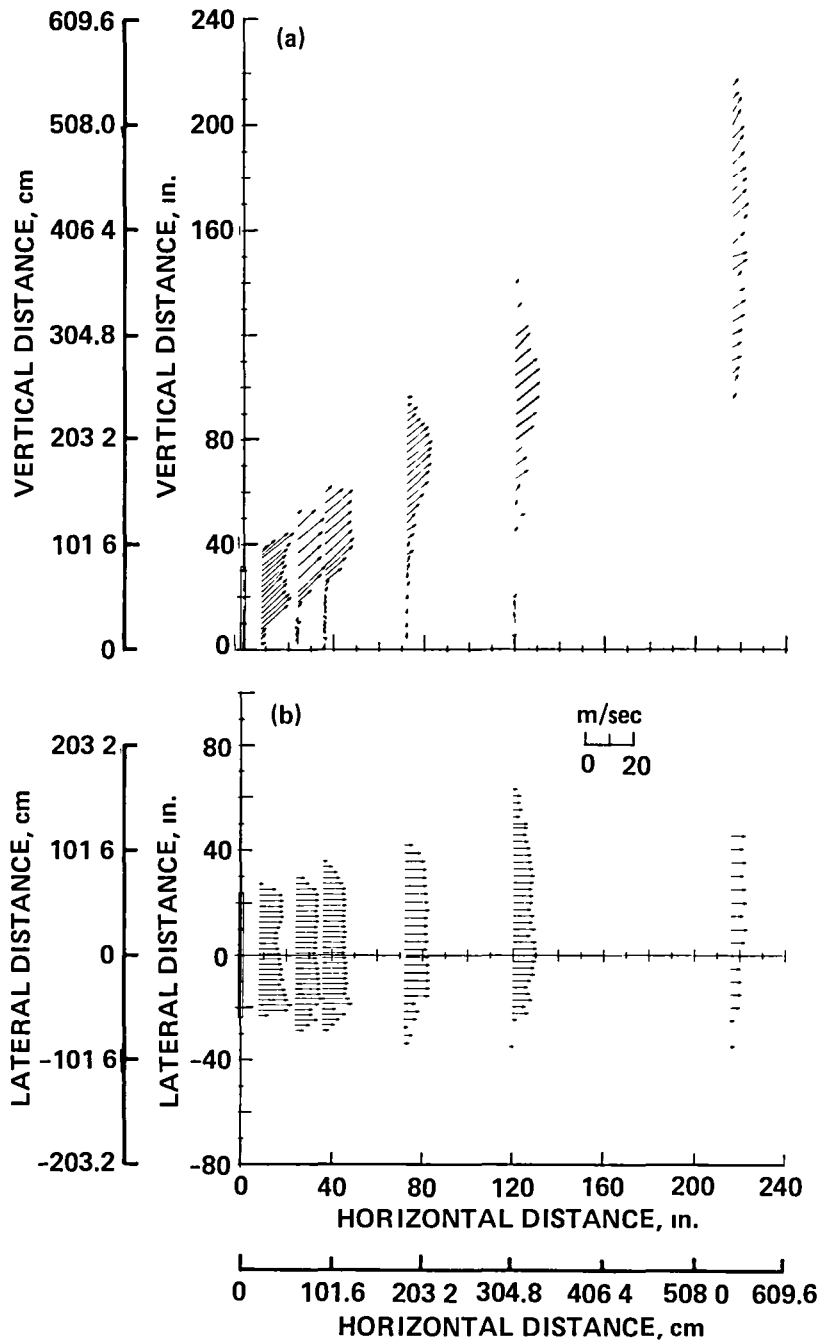porosity of about 30%. (c) Wire screen; porosity = 43%. (d) Wire screen (poros-
ity = 43%) with taped strips 0.635 cm (1/4 in.) wide spaced 1.27 cm (1/2 in.)
apart to yield an average porosity of about 29%.

32

Figure 20.- Vector representation of velocity in flow field downstream of exhaust opening with recommended ramp 15.24 cm (6 in.) long at 45° elevation and with 30% porosity created by 0.32 cm (1/8 in.) holes uniformly spaced; V_{ts} = 55 knots (28 m/sec). (a) Side view of velocity distributions along vertical traverses through centerplane of jet. (b) Top view of velocity distribution along horizontal traverses through center of jet.
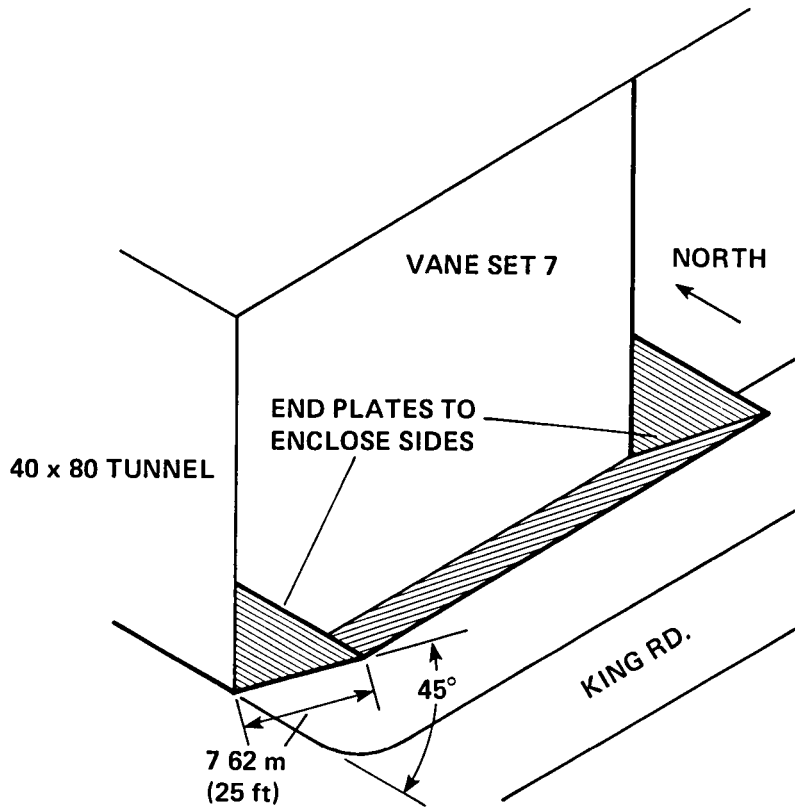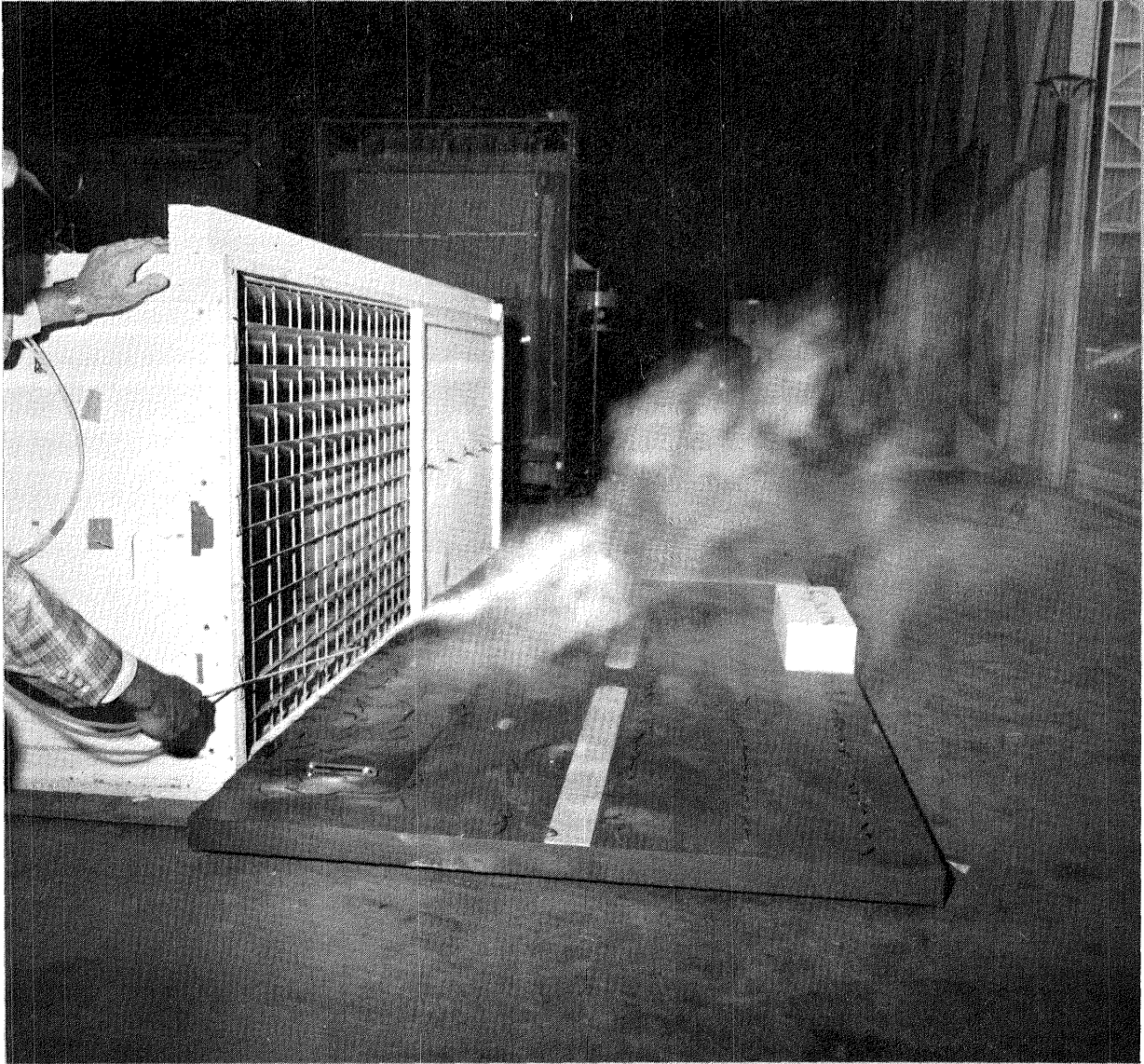
VANE SET 7

NORTH

END PLATES TO
ENCLOSE SIDES

40 x 80 TUNNEL
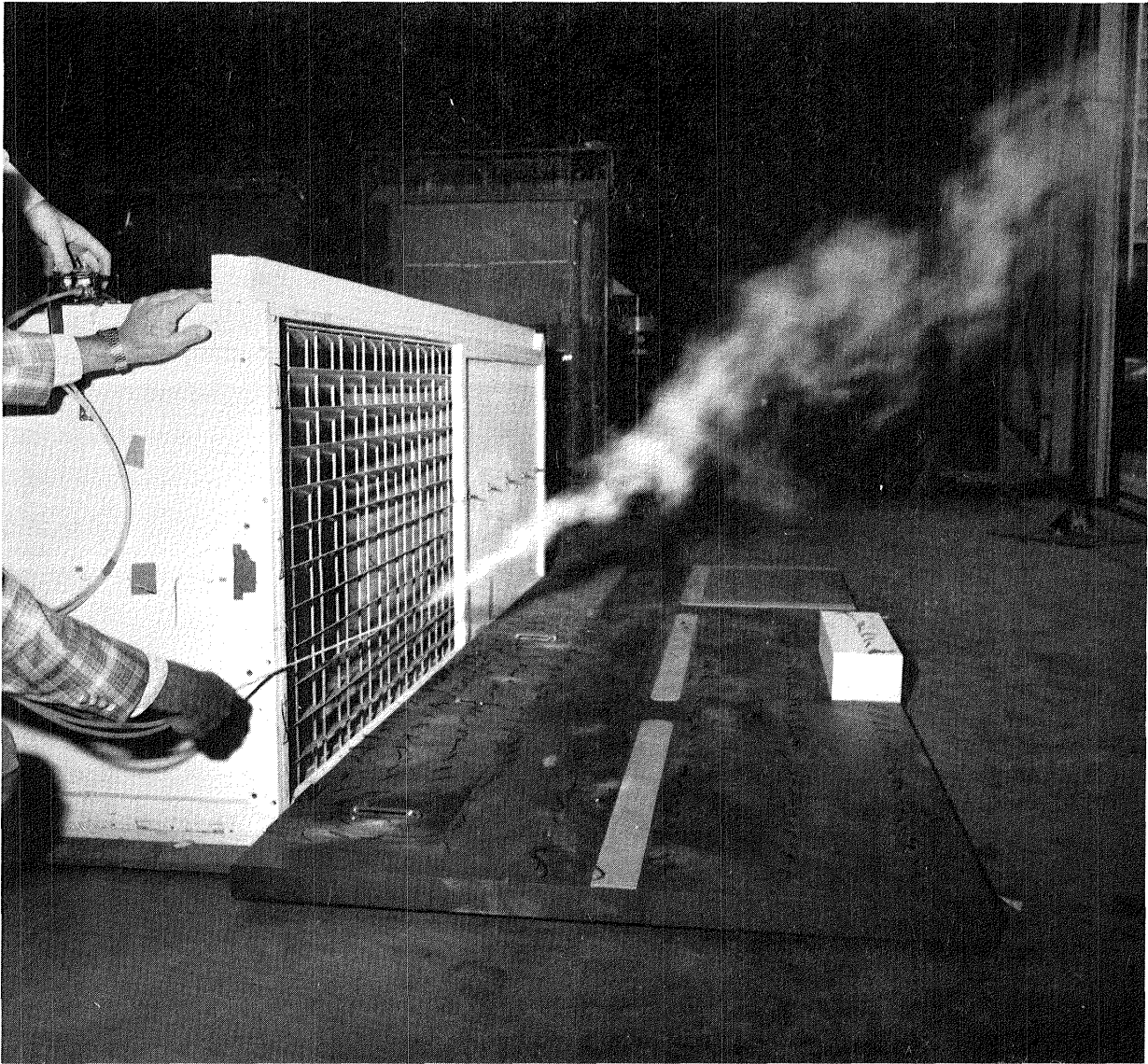
KING RD.

45°

7 62 m
(25 ft)

Figure 21.- Diagram of ramp area to illustrate how end plates are to be made.

(a) Smoke injected at lower edge of opening to illustrate how flow stays attached to ground plane. (AC83-8013-41)

Figure 22.- Photographs of smoke trails in exhaust of 1/50th scale model of 80- by 120-Foot Wind Tunnel when no deflector ramp is present.

(b) Smoke injected part way up exhaust opening to illustrate that jet flow is gener-
ally upward but that considerable turbulence exists as evidenced by sinuous form
of smoke trail. (AC83-8013-42)

Figure 22.- Concluded.
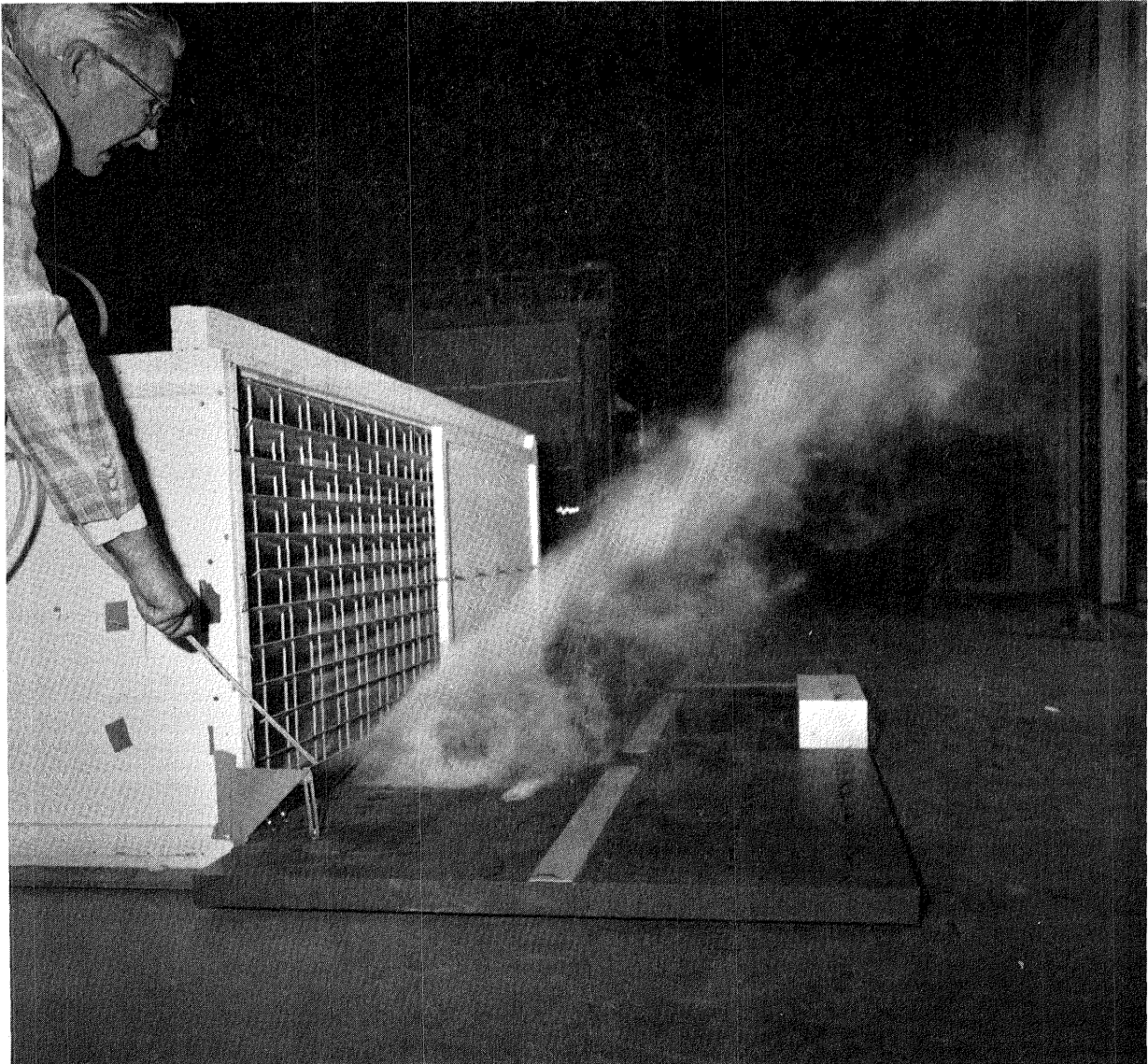
(a) Smoke injected at lower edge of ramp to illustrate nearly stagnant region under ramp. (AC83-8013-34)

Figure 23.- Photographs of smoke trails in exhaust of 1/50th scale model of 80- by 120-Foot Wind Tunnel when recommended ramp 15.24 cm (6 in.) long at 45° elevation and with 30% porosity created by uniformly spaced 0.32 cm (1/8 in.) diameter holes is present.
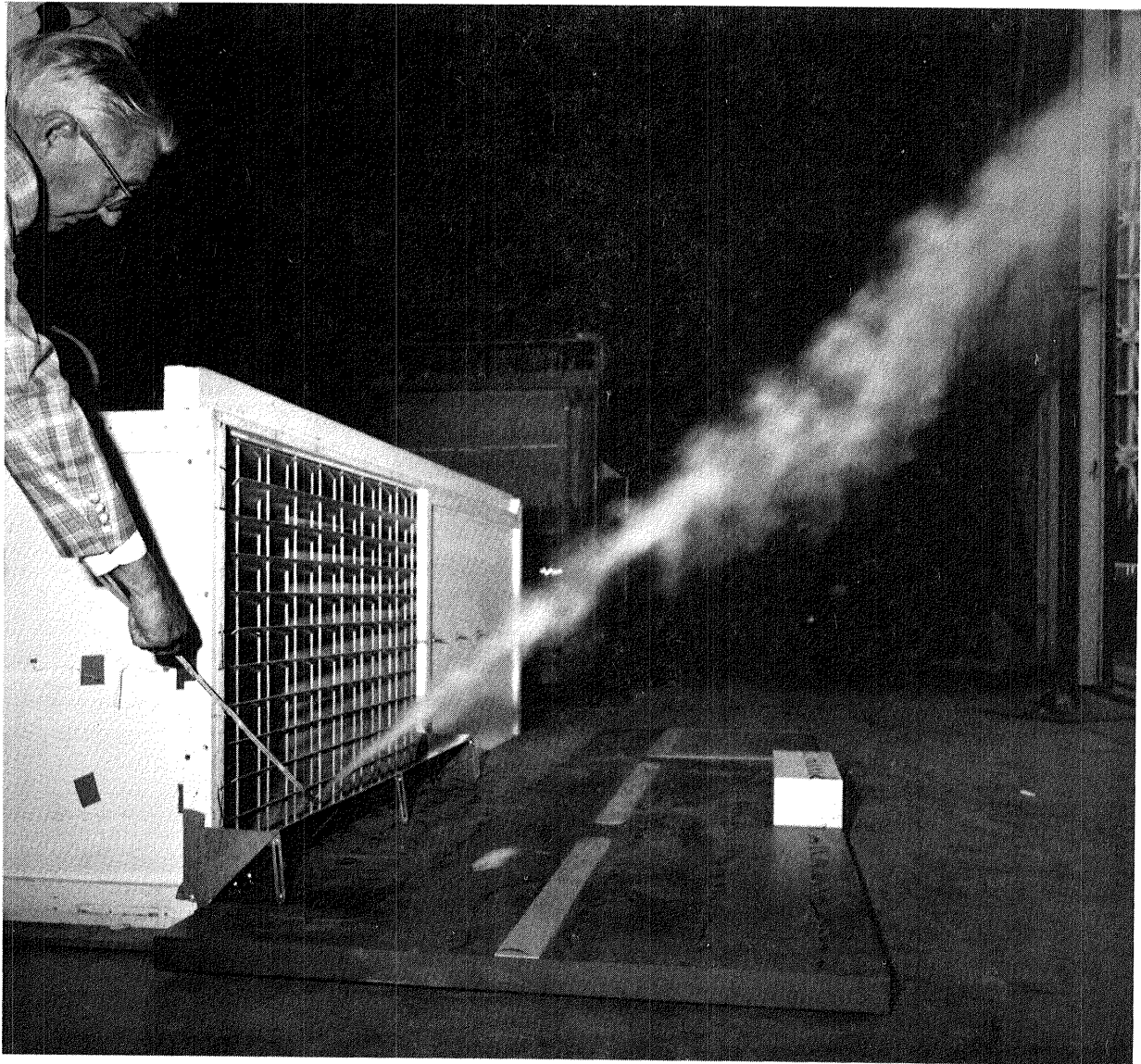
(b) Smoke injected slightly above ramp to illustrate how cleanly jet separates
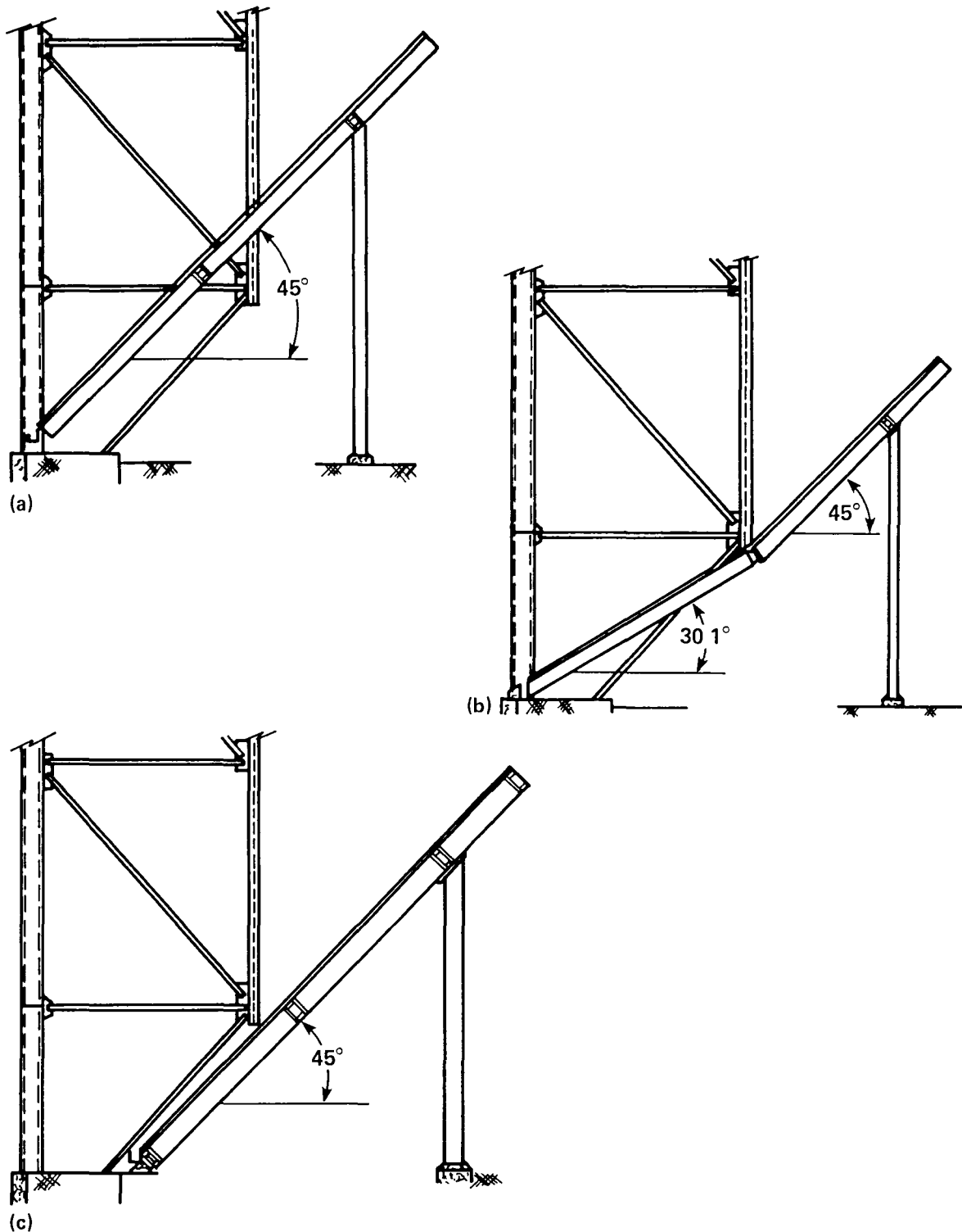from ground plane. (AC83-8013-33)

Figure 23.- Concluded.

Figure 24.- Diagrams of possible ways to incorporate ramp into and around external
structure of wind tunnel building. (a) Straight ramp beginning at lower edge of
exhaust opening. (b) Ramp beginning at lower edge of opening but bent slightly
to reduce interference with external structure of building. (c) Lower end of
ramp located far enough from building to avoid interference with structural
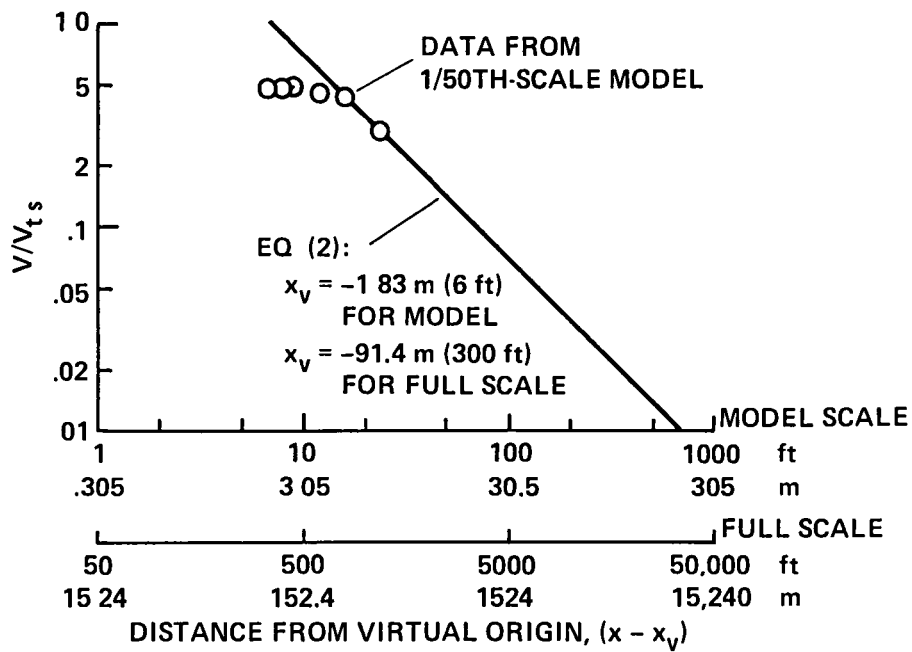steel. It is most likely one to be built full scale.

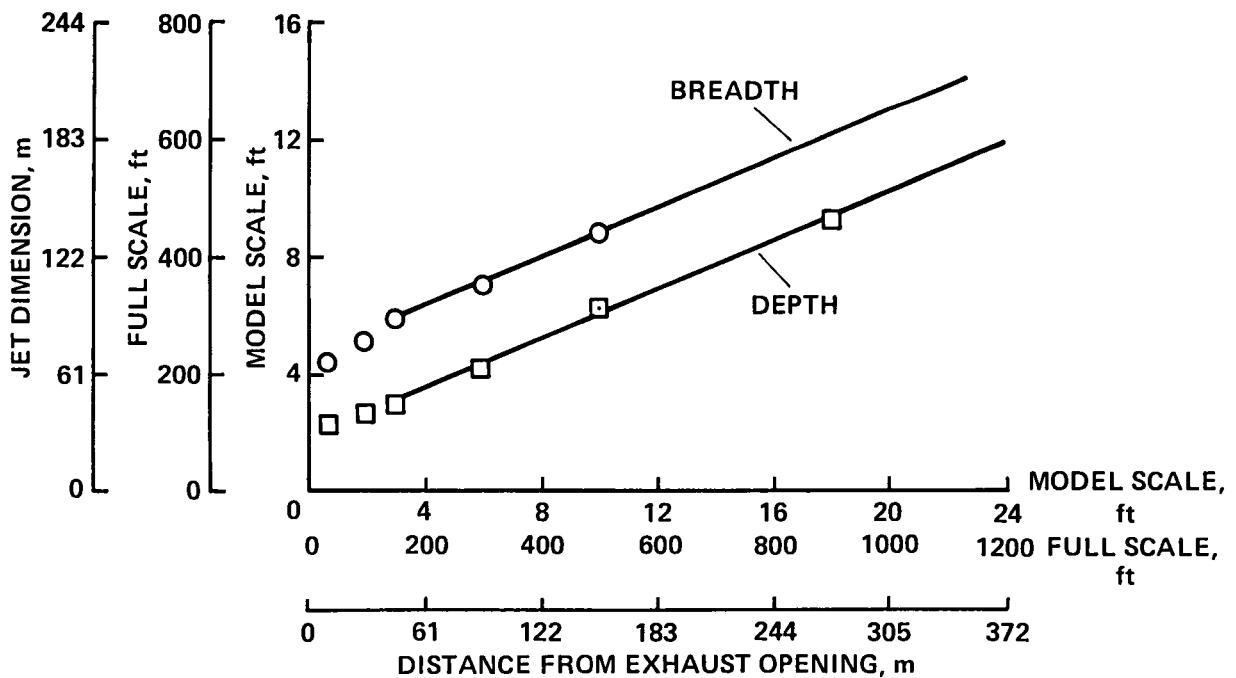Figure 25.- Variation of centerline velocity of jets with distance from virtual origin.

Figure 26.- Variation of depth and breadth of jet as a function of distance from virtual origin.

1 Report No NASA TM 88195	2 Government Accession No	3 Recipient's Catalog No	
4 Title and Subtitle EXPERIMENTAL STUDY OF FLOW DEFLECTORS DESIGNED TO ALLEVIATE GROUND WINDS INDUCED BY EXHAUST OF 80- BY 120-FOOT WIND TUNNEL		5 Report Date January 1986	
		6 Performing Organization Code	
7 Author(s) Vernon J. Rossow, Gene I. Schmidt, Michael S. Reinath, Johannes M. Van Aken (University of Kansas, Lawrence, KS 66044), Cynthia L. Parrish, and Raymond F. Schuler		8 Performing Organization Report No A-86055	
9 Performing Organization Name and Address Ames Research Center Moffett Field, CA 94035		10 Work Unit No	
		11 Contract or Grant No	
12 Sponsoring Agency Name and Address National Aeronautics and Space Administration Washington, DC 20546		13 Type of Report and Period Covered Technical Memorandum	
		14 Sponsoring Agency Code 505-31-21	

15 Supplementary Notes

Point of Contact. Vernon J. Rossow, Ames Research Center, M/S 247-1, Moffett Field, CA 94035, (415) 694-6681 or FTS 464-6681

16 Abstract

A description is presented of an experimental study directed at finding a deflector ramp that will reduce to an acceptable level the ground winds under the exhaust jet of the 80- by 120-Foot Wind Tunnel at NASA Ames Research Center. A one-fiftieth scale model of the full-scale facility was used to investigate how the jet flow field was modified by the various design parameters of the ramp. It was concluded that the ground winds were alleviated sufficiently by a ramp with end plates located next to the wind tunnel building along the ground edge of the exhaust opening. At full scale, the ramp should have a slant length of 7.62 m (25 ft) or more, and would be elevated at about 45° to the ground plane. The material should have holes less than 15.2 cm (6 in.) in diameter distributed uniformly over its surface to produce a porosity of about 30%.

17 Key Words (Suggested by Author(s)) Wind-tunnel design Exhaust deflector	18 Distribution Statement Unlimited Subject category - 02		
19 Security Classif (of this report) Unclassified	20 Security Classif (of this page) Unclassified	21 No of Pages 42	22 Price* A03

End of Document